

✓ m (2)

# NAVAL POSTGRADUATE SCHOOL Monterey, California

AD-A243 793



DTIC  
ELECTE  
DEC 31 1991  
S D D

## THESIS

PLANE WAVE SCATTERING FROM CIRCULAR AND  
HOLLOW CIRCULAR SLIT CYLINDERS USING THE  
ON-SURFACE RADIATION  
CONDITION (OSRC) APPROACH

by

Syed Mahmood Ali

December 1990

Thesis Advisor: Ramakrishna Janaswamy

Approved for public release; distribution is unlimited

91-19139



91 1227-011

UNCLASSIFIED

SECURITY CLASSIFICATION OF THIS PAGE

REPORT DOCUMENTATION PAGE				Form Approved OMB No. 0704-0188	
1a REPORT SECURITY CLASSIFICATION <b>UNCLASSIFIED</b>			1b. RESTRICTIVE MARKINGS		
2a. SECURITY CLASSIFICATION AUTHORITY			3. DISTRIBUTION/AVAILABILITY OF REPORT Approved for public release; distribution is unlimited		
2b. DECLASSIFICATION/DOWNGRADING SCHEDULE					
4. PERFORMING ORGANIZATION REPORT NUMBER(S)			5. MONITORING ORGANIZATION REPORT NUMBER(S)		
6a. NAME OF PERFORMING ORGANIZATION Naval Postgraduate School		6b OFFICE SYMBOL (If applicable) EC	7a. NAME OF MONITORING ORGANIZATION Naval Postgraduate School		
6c. ADDRESS (City, State, and ZIP Code) Monterey, CA 93943-5000			7b. ADDRESS (City, State, and ZIP Code) Monterey, CA 93943-5000		
8a. NAME OF FUNDING/SPONSORING ORGANIZATION		8b. OFFICE SYMBOL (If applicable)	9. PROCUREMENT INSTRUMENT IDENTIFICATION NUMBER		
8c. ADDRESS (City, State, and ZIP Code)			10. SOURCE OF FUNDING NUMBERS		
			PROGRAM ELEMENT NO.	PROJECT NO.	TASK NO.
			WORK UNIT ACCESSION NO.		
11 TITLE (Include Security Classification) PLANE WAVE SCATTERING FROM CIRCULAR AND HOLLOW CIRCULAR SLIT CYLINDERS					
12. PERSONAL AUTHOR(S) ALI, Syed Mahmood					
13a. TYPE OF REPORT Master's Thesis		13b. TIME COVERED FROM _____ TO _____		14. DATE OF REPORT (Year, Month, Day) 1990 December	15. PAGE COUNT 80
16 SUPPLEMENTARY NOTATION The views expressed in this thesis are those of the author and do not reflect the official policy or position of the Department of Defense or the US Government.					
17 COSATI CODES			18. SUBJECT TERMS (Continue on reverse if necessary and identify by block number)		
FIELD	GROUP	SUB-GROUP	surface radiation conditions; transverse electric; circular cylinders; hollow cylinder slit cylinders		
19 ABSTRACT (Continue on reverse if necessary and identify by block number)					
A new formulation of electromagnetic wave scattering by convex, two dimensional conducting bodies was introduced by Kriegsman et all in ref. [1]. This formulation, called the On Surface Radiation Condition (OSRC) approach is based upon an expansion of the radiation condition applied directly on the surface of the scatterer. Past approaches involved applying a radiation condition at some distance from the scatterer in order to achieve a nearly reflection free truncation of a finite difference time domain lattice. Application of a suitable radiation condition directly on the surface of the convex conducting scatterer can lead to substantial simplification of the frequency domain integral equation for the scattered field, which is reduced to just a line integral. In this thesis, the application of the second order radiation boundary condition of ref.[1] to					
20 DISTRIBUTION/AVAILABILITY OF ABSTRACT <input checked="" type="checkbox"/> UNCLASSIFIED/UNLIMITED <input type="checkbox"/> SAME AS RPT <input type="checkbox"/> DTIC USERS			21 ABSTRACT SECURITY CLASSIFICATION <b>UNCLASSIFIED</b>		
22a. NAME OF RESPONSIBLE INDIVIDUAL JANASWAMY, Ramakrishna		22b. TELEPHONE (Include Area Code) 408-646-3217		22c. OFFICE SYMBOL EC/Js	

DD Form 1473, JUN 86

Previous editions are obsolete

SECURITY CLASSIFICATION OF THIS PAGE

S/N 0102-LF-014-6603

UNCLASSIFIED

19. cont.

concave and re-entrant two dimensional bodies is considered. The specific shapes considered are slit circular cylinders and thick semi-circular cylinders. The formulation is done for the more challenging case of Transverse Electric (TE) polarization. The bodies considered here are two dimensional in nature and are perfectly conducting. Results are presented for the surface current distribution and scattering width of these cylinders and comparison is made with known results. It was found that the OSRC approach may not be applicable to concave structures and also for higher values of  $kb$  for convex bodies.

Approved for public release; distribution is unlimited.

**Plane Wave Scattering from Circular and Hollow  
Circular Slit Cylinders using the On Surface  
Radiation Condition Approach**

**Syed Mahmood Ali**  
Lieutenant commander Pakistan Navy  
B.S.E.E., University of Karachi, 1976

Submitted in partial fulfillment  
of the requirements for the degree of

MASTER OF SCIENCE IN ELECTRICAL AND COMPUTER ENGINEERING

from the

NAVAL POSTGRADUATE SCHOOL  
December 1990



Author:

Syed Mahmood Ali

Approved by:

Ramakrishna Janaswamy, Thesis Advisor

Richard W. Adler, Second Reader

Michael A. Morgan, Chairman,  
Department of Electrical and Computer engineering

Accession For	
NTIS CRA&I	<input checked="" type="checkbox"/>
DTIC TAB	<input type="checkbox"/>
Unannounced	<input type="checkbox"/>
Justification	
By	
Distribution	
Availability Codes	
Date	Availability Statement
A-1	

## ABSTRACT

A new formulation of electromagnetic wave scattering by convex, two dimensional conducting bodies was introduced by Kriegsman et al in ref.[1]. This formulation, called the On Surface Radiation Condition (OSRC) approach is based upon an expansion of the radiation condition applied directly on the surface of the scatterer. Past approaches involved applying a radiation condition at some distance from the scatterer in order to achieve a nearly reflection free truncation of a finite difference time domain lattice. Application of a suitable radiation condition directly on the surface of the convex conducting scatterer can lead to substantial simplification of the frequency domain integral equation for the scattered field, which is reduced to just a line integral. In this thesis, the application of the second order radiation boundary condition of ref.[1] to concave and re-entrant two dimensional bodies is considered. The specific shapes considered are slit circular cylinders and thick semi-circular cylinders. The formulation is done for the more challenging case of Transverse Electric (TE) polarization. The bodies considered here are two dimensional in nature and are perfectly conducting. Results are presented for the surface current distribution and scattering width of these cylinders and comparison is made with known results. It was found that the OSRC approach may not be applicable to concave structures and also for higher values of  $kb$  for convex bodies.

## TABLE OF CONTENTS

I.	INTRODUCTION -----	1
II.	SCATTERING FROM CIRCULAR CYLINDERS FOR THE TE CASE:	
	OSRC APPROACH -----	3
	A. GENERAL FORMULATION FOR THE TE CASE -----	3
	B. APPLICATION TO CIRCULAR CYLINDERS -----	7
	1. SOLUTION OF THE DIFFERENTIAL EQUATION FOR THE	
	SURFACE SCATTERED FIELD -----	9
	2. SURFACE CURRENT DISTRIBUTION -----	12
	3. FAR ZONE SCATTERED FIELDS -----	13
III.	SCATTERING FROM SLIT CIRCULAR CYLINDERS: OSRC	
	APPROACH -----	16
	A. DETERMINATION OF SURFACE CURRENTS -----	16
	B. DETERMINATION OF THE FAR FIELDS -----	19
IV.	NUMERICAL RESULTS AND DISCUSSION -----	27
V.	CONCLUSIONS -----	41
APPENDIX A:	COMPUTER PROGRAM TO COMPUTE CURRENT DISTRIBUTION	
	FOR CIRCULAR CYLINDERS -----	42
APPENDIX B:	COMPUTER PROGRAM TO COMPUTE NORMALIZED SCATTERING	
	WIDTH $\sigma/b$ FOR CIRCULAR CYLINDERS -----	44
APPENDIX C:	COMPUTER PROGRAM TO COMPUTE $\sigma/\pi b$ Versus $kb$ FOR	
	CIRCULAR CYLINDERS -----	46
APPENDIX D:	COMPUTER PROGRAM TO COMPUTE $J_s$ FOR SLIT CIRCULAR	
	CYLINDERS -----	48

APPENDIX E: COMPUTER PROGRAM TO COMPUTE $\sqrt{\sigma/\lambda}$ versus $\phi$ FOR SLIT CIRCULAR CYLINDERS -----	50
APPENDIX F: COMPUTER PROGRAM TO COMPUTE $\sigma/\pi b$ versus $kb$ FOR CIRCULAR SLIT CYLINDERS -----	56
APPENDIX G: PROGRAM TO COMPUTE THE BESSEL FUNCTIONS -----	62
APPENDIX H: PROGRAM TO COMPUTE THE INTEGRATION ROUTINES --	66
LIST OF REFERENCES -----	68
INITIAL DISTRIBUTION LIST -----	70

## ACKNOWLEDGEMENTS

I would like to express my sincere appreciation to my thesis advisor, Professor Ramakrishna Janaswamy. Without his assistance, this thesis could not have been undertaken. His outstanding professional competence, timely advice and friendly attitude made all the difference.

I am also thankful to Professor Michael A. Morgan who allowed me to use his research area and computer setup. Finally, I would like to thank my wife, Bina, my two sons, Danish and Sameer, and my daughter, Sonia, for their support, love and patience during the entire stay in the United States.

## I. INTRODUCTION

The On-Surface Radiation Condition (OSRC) approach presented here is a medium frequency technique for modeling electromagnetic scattering from complex bodies. It is based upon an expansion of the radiation condition applied directly on the surface of the scatterer. Past techniques involved applying a radiation condition at some distance from the scatterer in order to achieve a nearly reflection free truncation of a finite time domain lattice. Application of a suitable radiation condition directly on the surface of the scatterer can lead to substantial simplification of the frequency domain integral equation for the scattered field, which is reduced to just a line integral. The OSRC technique converts the usual surface integral equation for the scattering problem into either an integration of unknown quantities or a simple ordinary differential equation for convex two-dimensional objects. For the Transverse Electric (TE) case, the problem reduces to solving an ordinary differential equation around the scatterer contour and for the Transverse Magnetic (TM) case, the solution is known explicitly. It is currently applicable to convex conducting cylinders of arbitrary cross sections for both TE and TM cases. The OSRC approach was motivated, as mentioned in ref. [1], by numerical experiments conducted over the past

twenty years aimed at simulating scalar or vector wave propagation and scattering using a finite difference time domain (FD-TD) model of the governing wave equation.

In the subsequent sections of this thesis, we will use the OSRC theory to study scattering by two dimensional, convex and concave shaped conducting scatterers for the TE case. The specific shapes considered are the slit circular cylinder and the thick semi-circular cylinder. More emphasis is placed on the TE case using the second order boundary condition. Results and comparisons are shown for the TE case. Comparisons of current distributions for circular cylinders with normalized circumferences ( $kb$ ) of 5 and 10 with ref.[1] are made. Also comparisons of bistatic cross sections for circular cylinders are made for several values of  $Kb$ . For the thick semi-circular cylinder and the slit cylinders, comparison is shown for the induced current density and the normalized scattering width.

## II. SCATTERING FROM CIRCULAR CYLINDERS: OSRC APPROACH

In this chapter we will first apply the OSRC technique to two dimensional, perfectly conducting and convex shaped cylinders. Next we will apply the second order boundary conditions to circular cylinders with radius  $r_0$  and obtain a second order differential equation for the surface scattered field. The differential equation is solved by the Fourier series method. Finally expressions are obtained for the surface current distribution and the scattered fields.

### A. GENERAL FORMULATION FOR THE TE POLARIZATION CASE

This formulation is based on the second order radiation conditions mentioned in ref. [1]. For the TE polarization case, the problem reduces to solving an ordinary differential equation around the scatterer surface contour.

Consider a plane electromagnetic wave illuminating a two dimensional, perfectly conducting, convex shaped cylinder for the TE polarization case. The incident wave, propagating at an angle  $\alpha$  with respect to the  $-x$  axis (see Fig. 1), is given by

$$H_{inc} = U_{inc} e^{j\omega t} \hat{z} ; \quad U_{inc} = e^{-jk(x\cos\alpha - y\sin\alpha)} \quad (1)$$

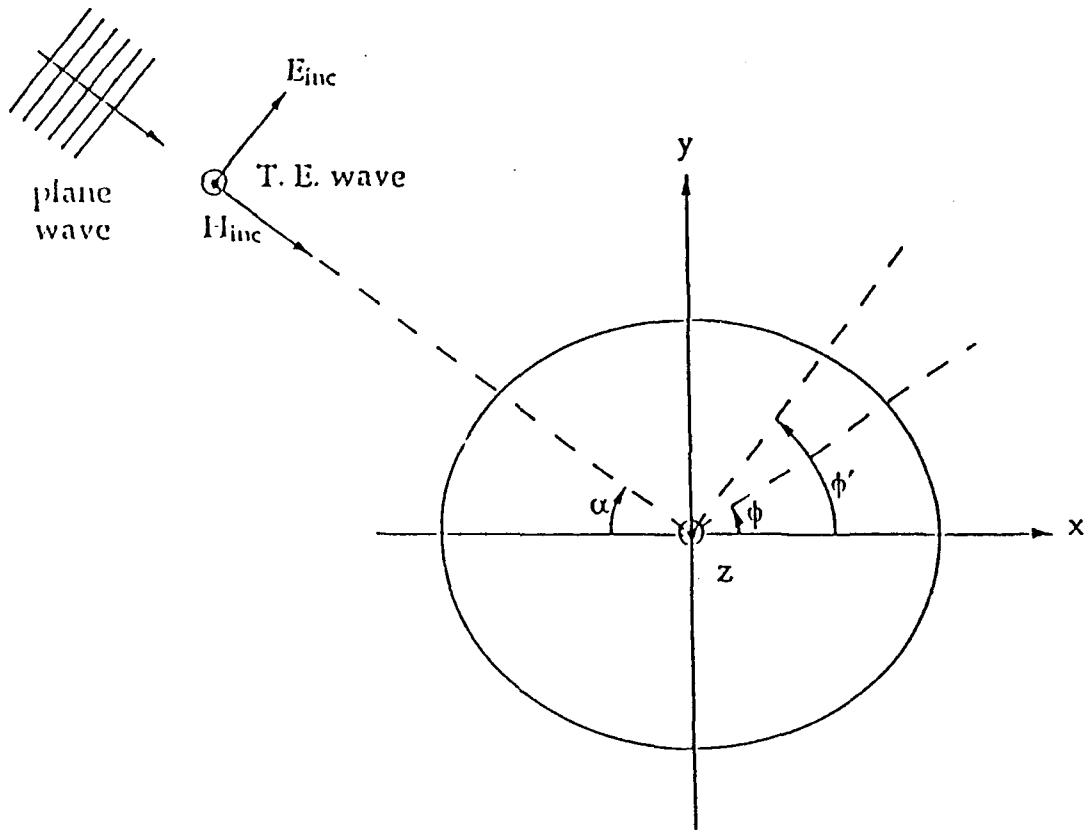


**Fig.1 TE incident field**

where  $\hat{z}$  is the unit vector parallel to the cylinder axis;  $\omega$  is the frequency of the incident wave ( $k = \omega/c$ );  $c$  is the speed of light in free space;  $x$  and  $y$  are the corresponding cartesian coordinates in the plane orthogonal to  $\hat{z}$ .

Since the problem is two dimensional, the scattered magnetic field (see Fig.2) is assumed to be



$$G(\bar{r}/\bar{r}') = \frac{1}{4j} H_0^{(2)}(kR) \quad (4)$$

$$R = |\bar{r} - \bar{r}'| = \sqrt{(x-x')^2 + (y-y')^2} \quad (5)$$

$\bar{r}$  and  $\bar{r}'$  are co-ordinates of the field and source points, i.e.  $\bar{r} = (x, y)$  and  $\bar{r}' = (x', y')$ , and  $s'$  is the arc length parameter.

For the TE case, vanishing of the total tangential electric field on the surface of the cylinder produces

$$\frac{\partial U_s}{\partial v'} = - \frac{\partial U_{inc}}{\partial v'}$$

The objective is to determine  $U_s$  on the surface of the scatterer. For later purposes, it is necessary to obtain an expression for the far-zone fields. Using the asymptotic form of the Hankel function it can be shown that the far-zone scattered field is

$$U_s \sim B_o \frac{e^{-jkx}}{\sqrt{x}} \quad (7)$$

with

$$B_o = \frac{e^{j\pi/4}}{\sqrt{8k\pi}} \int_c \left[ \frac{\partial U_s}{\partial v'} + jk \cos \delta U_{inc} \right] e^{jkx' \cos \psi} ds' \quad (8)$$

where

$$\cos \delta = \hat{v}' \cdot \hat{f} \quad \text{and} \quad \cos \psi = (\bar{r}' \cdot \hat{f})$$

The true fields satisfy Sommerfeld's radiation condition (ref.[6]) on an infinitely large outer cylinder. However, in the OSRC technique, a higher order boundary condition such as

$B_2$  (defined below) is applied directly on the surface of the object. Implicit in this approximation is the fact that only outgoing waves are assumed to exist on the surface. Thus, the approximation is expected to have serious drawbacks in geometries where significant stored energy can exist such as in re-entrant and slit cylinders. In the sections to follow, we will be dealing precisely with these situations.

The form of second order boundary condition  $B_2$  is given from (ref.[1]) with  $-jk$  in place of  $jk$  as

$$\left[ -jk - \frac{\zeta(s')}{2} + \frac{\zeta^2(s')}{8[jk + \zeta(s')]} \right] + \frac{1}{2[jk + \zeta(s')]} \frac{\partial^2}{\partial s'^2} - \frac{\partial}{\partial v'} , \quad (9)$$

where  $\zeta(s')$  is the curvature of the surface at  $s'$ .

The condition  $B_2 U_s = 0$  is applied to circularly shaped cylinders in the next section.

## B. APPLICATION TO CIRCULAR CYLINDERS

At the surface of the perfect electric conductor, the boundary conditions on the total fields state that

$$\hat{n} \times \vec{H} = \vec{J}_s ; \quad \hat{n} \times \vec{E} = 0 \quad (10)$$

where  $J_s$  is the total surface current. For the TE case the scattered fields  $(\vec{E}^s, \vec{H}^s)$  are

$$H_z^s = U_s \quad \text{and} \quad E_\phi^s = -\frac{1}{j\omega\mu_0} \frac{\partial U_s}{\partial v'} . \quad (11)$$

Hence we have  $\partial(U_{inc} + U_s)/\partial v' = 0$  and  $J_\phi = -(U_s + U_{inc})$  on the surface, where  $v'$  is positive for convex surfaces and negative for concave surfaces.

For  $\alpha = 0$  in (1), the normal derivative of  $U_s$  can be rewritten as

$$\frac{\partial U_s}{\partial v'} = -\frac{\partial U_{inc}}{(\pm)\partial r'} = (\pm) -\frac{\partial}{\partial r'} (e^{-jkr'\cos\phi'}) = \pm jk\cos\phi' U_{inc} . \quad (12)$$

Substituting the expression for  $J_\phi$  and (12) in (9), setting the curvature  $\zeta(s')$  equal to  $1/r_0$ , and replacing  $\frac{\partial^2}{\partial s'^2}$  by  $\frac{1}{r^2} \frac{\partial^2}{\partial \phi'^2}$

gives

$$C_2 \frac{\partial^2 J_\phi}{\partial \phi'^2} - J_\phi = U_{inc} (1 - C_1 \cos\phi) - C_2 \frac{\partial^2 U_{inc}}{\partial \phi'^2} , \quad (13)$$

where

$$C_1 = \pm \frac{8k^2 r_0^2 - 8jkr_0}{8k^2 r_0^2 - 12jkr_0 - 3} \quad \text{and} \quad C_2 = -\frac{4}{8k^2 r_0^2 - 12jkr_0 - 3} . \quad (14)$$

In  $C_1$ , the upper sign is valid for convex surfaces and the lower one for concave surfaces. The above equation is valid on the surface  $r' = r_0$  with  $J_\phi$  being  $2\pi$  periodic. Equation (13) is

linear with constant coefficients and can be solved using standard analytical or numerical methods. Analytical methods such as the method of undetermined coefficients and variation of parameters yielded complicated integrals for the solution of the second order non-homogeneous differential equation (13). Therefore (13) was solved using a Fourier series expansion.

### 1. SOLUTION OF THE DIFFERENTIAL EQUATION FOR THE SURFACE SCATTERED FIELD

Rewriting (11) in terms of  $U_s$  gives

$$C_2 \frac{\partial^2 U_s}{\partial \phi^2} - U_s = C_1 \cos \phi' U_{inc} . \quad (15)$$

The incident field on the surface of the cylinder is

$$U_{inc}|_{r'=r_0} = e^{-jkr' \cos \phi'} \quad (16)$$

which may be expressed in a Fourier series as (ref.[6])

$$U_{inc}|_{r'=r_0} = \sum_{-\infty}^{\infty} j^{-n} J_n(kr_0) e^{jn\phi'} . \quad (17)$$

We will assume a complex exponential form for the Fourier series representation of  $U_s$ ,

$$U_s = \sum_{n=-\infty}^{\infty} A_n e^{jn\phi} . \quad (18)$$

The coefficient  $A_n$  will be solved by substituting into equation (15). For  $U_s$  on the circular portion of the cylinder, we have

$$\frac{\partial U_s}{\partial \phi} = j \sum_{n=-\infty}^{\infty} n A_n e^{jn\phi} \quad (19)$$

and

$$\frac{\partial^2 U_s}{\partial \phi^2} = - \sum_{n=-\infty}^{\infty} n^2 A_n e^{jn\phi} . \quad (20)$$

Substituting these into the Left Hand Side (LHS) of (15), we get

$$LHS = - \sum_{n=-\infty}^{\infty} (C_2 n^2 + 1) A_n e^{jn\phi} . \quad (21)$$

Now expanding the Right Hand Side (RHS) of (15),

$$\begin{aligned} C_1 U_{inc} \cos \phi' &= C_1 \sum_{n=-\infty}^{\infty} j^{-n} J_n(kr_o) e^{jn\phi} \frac{1}{2} (e^{j\phi'} + e^{-j\phi'}) \\ &= \frac{C_1}{2} \left[ \sum_{n=-\infty}^{\infty} j^{-n} J_n(kr_o) e^{j(n+1)\phi'} + \sum_{n=-\infty}^{\infty} j^{-n} J_n(kr_o) e^{j(n-1)\phi'} \right] . \quad (22) \end{aligned}$$

We now let  $n+1=m \rightarrow n=m-1$  in the first series and  $n-1=m \rightarrow n=m+1$  in the second to obtain

$$RHS = -C_1 \sum_{j=-\infty}^{\infty} j^{-(m+1)} e^{j m \psi} J'_m(kr_o). \quad (23)$$

In obtaining (23), use was made of the expression  $2J'_m(Kr_o) = J'_{m-1}(Kr_o) - J'_{m+1}(Kr_o)$ . Equating the coefficients of (21) and (23) yields the following expression for the Fourier series coefficient  $A_n$ ,

$$A_n(r_o) = \frac{C_1 j^{-(n+1)} J'_n(kr_o)}{1 + C_2 n^2}. \quad (24)$$

We note that the coefficients are dependent on the radius  $r_o$  of the cylindrical surface. For numerical calculations, the series in (18) needs to be truncated. For determining the truncation value of  $n$ , we determine  $A_n$  for large  $n$ . For large values of the order  $n$ , we have from ref. [10]

$$J_n(kr_o) \sim \frac{1}{\sqrt{2\pi n}} \left( \frac{ekr_o}{2n} \right)^n. \quad (25)$$

Also using the recurrence relation

$$J'_n(kr_o) = \frac{1}{2} [J_{n-1}(kr_o) - J_{n+1}(kr_o)], \quad (26)$$

we obtain for  $\frac{ekr_o}{2n} < 1$

$$J'_n(kr_o) \sim \frac{1}{2\sqrt{2\pi n}} \left(\frac{ekr_o}{2n}\right)^{n-1} . \quad (27)$$

Therefore for large  $n$ ,  $A_n$  can be expressed as

$$A_n \sim \frac{C_1}{C_2} j^{-(n+1)} \frac{1}{2\sqrt{2\pi}} \left(\frac{ekr_o}{2}\right)^{n-1} \left(\frac{1}{n}\right)^{\frac{5}{2}} . \quad (28)$$

Hence  $A_n$  decays very rapidly, for example

$$\frac{A_{10}}{A_1} \sim 10^{-11} .$$

## 2. SURFACE CURRENT DISTRIBUTION

Having found the surface magnetic field, it is a simple task to determine the surface current. The total electric surface current  $J_\phi$  for the circular cylinder is given by

$$J_\phi = -(U_s + U_{inc}) . \quad (29)$$

Substituting (17) and (18) in (29) gives

$$J_\phi = - \sum_{-\infty}^{\infty} [A_n + j^{-n} J_n(kr_o)] e^{jn\phi} . \quad (30)$$

After expanding and simplifying, (30) reduces to

$$J_{\phi} = -\sum_0^{\infty} \epsilon_n \left[ \frac{C_1 j^{-(n+1)} J'_n(kr_0)}{1+C_2 n^2} + j^{-n} J_n(kr_0) \right] \cos n\phi' , \quad (31)$$

where  $\epsilon_n = 1$  for  $n$  equal to zero and  $\epsilon_n = 2$  for  $n$  not equal to zero, and  $C_1$  and  $C_2$  are given in (14). However for  $C_1$  the positive sign is taken since the surface is convex. The magnitude of the normalized surface current can be expressed as

$$\left| \frac{J_{\phi}}{H_{inc}} \right| = \left| -\sum_0^{\infty} \epsilon_n j^{-n} \left[ \frac{C_1 j^{-1} J'_n(kr_0)}{1+C_2 n^2} + J_n(kr_0) \right] \cos n\phi' \right| . \quad (32)$$

### 3. FAR ZONE SCATTERED FIELDS

The far-zone scattered magnetic field  $H_z^s$  for the TE case given at (8) can also be expressed as (ref.[5] page 374)

$$H_z^s = \frac{e^{-jkR}}{\sqrt{r}} \frac{j}{4} \left( \frac{2j}{\pi k} \right)^{\frac{1}{2}} \int_C [e^{jk\hat{r} \cdot \hat{r}'} \frac{\partial H_z^s}{\partial v'} - H_z^s(\hat{r}, \phi')] j k e^{jk\hat{r} \cdot \hat{r}'} dC' , \quad (33)$$

where  $C$  is a closed contour around the cylinder.

In our case, with reference to Fig.2, we have

$$e^{jkz} \cdot \vec{r}' = e^{jkr_o \cos \psi} = e^{jkr_o \cos(\psi' - \psi)} , \quad (34)$$

$$H_z^s = U_s = \sum_{-\infty}^{\infty} A_n e^{jn\psi'} , \quad (35)$$

$$(\hat{r} \cdot \psi') = \pm \cos(\psi' - \psi) , \quad (36)$$

$$\frac{\partial H_z^s}{\partial \psi'} = \mp k \sum_{-\infty}^{\infty} j^{-n} J_n'(kr_o) e^{jn\psi'} . \quad (37)$$

Substituting (34) through (37) in (33) and simplifying we get

$$H_z^s = -k \frac{e^{-jkz}}{\sqrt{r}} \frac{j}{4} \left( \frac{2j}{\pi k} \right)^{\frac{1}{2}} r_o \left[ \sum_{-\infty}^{\infty} j^{-n} J_n'(kr_o) \int_c e^{jkr_o \cos(\psi' - \psi)} \cdot e^{jn\psi'} d\psi' + \frac{1}{k} \sum_{-\infty}^{\infty} A_n \frac{\partial}{\partial r'} \Big|_{r'=r_o} \left( \int_c e^{jkr' \cos(\psi' - \psi)} e^{jn\psi'} d\psi' \right) \right] . \quad (38)$$

In the derivation of the above equation, we made use of the fact that  $j k \cos(\psi' - \psi) e^{jkr_o \cos(\psi' - \psi)} = \frac{\partial}{\partial r'} \Big|_{r'=r_o} (e^{jkr_o \cos(\psi' - \psi)})$ .

For a full cylinder we can further simplify equation (38) by solving the integral portion as

$$\int_0^{2\pi} e^{jkr_o \cos(\psi' - \psi)} e^{jn\psi'} d\psi' = (-1)^n 2\pi e^{\frac{-jn\pi}{2}} e^{jn\psi} J_n(kr_o) . \quad (39)$$

Substituting the above value in (38) and after some manipulation, we get

$$H_z^s = -k \frac{e^{jkx}}{\sqrt{r}} \frac{j}{4} \left( \frac{2j}{\pi k} \right)^{\frac{1}{2}} r_o [2\pi \epsilon_n [\mathcal{J}'_n(kr_o) \mathcal{J}_n(kr_o) + j^n A_n \mathcal{J}'_n(kr_o)] \cos n\phi] \quad (40)$$

We list below a summary of the various quantities that were determined in this chapter.

$$\begin{aligned} \text{Surface scattered field... } U_s|_{r'=r_o} &= \frac{\sum_{-\infty}^{\infty} C_1 j^{-(n+1)} \mathcal{J}'_n(kr_o) e^{jn\phi}}{1+C_2 n^2} \\ \text{Total surface field... } U_t|_{r'=r_o} &= -\sum_{-\infty}^{\infty} [A_n + j^{-n} \mathcal{J}_n(kr_o)] e^{jn\phi} \\ \text{Surface current... } J_\phi &= -\sum_{-\infty}^{\infty} [A_n + j^{-n} \mathcal{J}_n(kr_o)] e^{jn\phi} \end{aligned}$$

$$\begin{aligned} \text{Fourier coefficient... } A_n &= \frac{C_1 j^{-(n+1)} \mathcal{J}'_n(kr_o)}{1+C_2 n^2} \\ &\sim \frac{C_1}{C_2} j^{-(n+1)} \frac{1}{2\sqrt{2\pi}} \left( \frac{eKr_o}{2n} \right)^{n-1} \left( \frac{1}{n} \right)^{\frac{5}{2}} \\ \text{Far fields... } H_z^s &= -k \frac{e^{-jKr}}{\sqrt{r}} \frac{j}{4} \left( \frac{2j}{\pi k} \right)^{\frac{1}{2}} r_o \left[ \sum_{-\infty}^{\infty} j^{-n} \mathcal{J}'_n(kr_o) \int_C e^{jkr_o \cos(\psi-\phi)} \right. \\ &\quad \left. \cdot e^{jn\phi} d\phi' + \frac{1}{k} \sum_{-\infty}^{\infty} A_n \frac{\partial}{\partial r'} \Big|_{r'=r_o} \left( \int_C e^{jkr' \cos(\psi-\phi')} e^{jn\phi'} d\phi' \right) \right] \end{aligned}$$

In the next chapter we will develop expressions for the case when the cylinder is comprised of more than one circular surface.

### III. SCATTERING FROM CIRCULAR SLIT CYLINDERS: OSRC APPROACH

In this chapter we will consider the case of a slit cylinder with finite wall thickness. It is assumed that the thickness of the wall is electrically small so that the fields do not vary along it. Furthermore, we ignore the effect of the edges. Fig.3 shows the geometry of the slit circular cylinder. On the outer surface  $C_1$ , the body is convex, while on the inner surface  $C_3$  it is concave. Since both outward and inward travelling waves can exist in the interior region, and since the OSRC technique assumes waves of only one kind, it is not expected to yield correct results for the geometry. We will use the results developed in the previous sections for the circular surfaces. To distinguish between the outer and inner surface we shall use superscripts (**b** for the outer radius and **a** for the inner radius) for the Fourier coefficients.

#### A. DETERMINATION OF SURFACE CURRENTS

The expression for the current distribution is given in (29) i.e.  $J_\phi = -(U_s + U_{inc})$ , where

$$U_s = \sum_{-\infty}^{\infty} A_n e^{jn\phi} \quad (41)$$

and

$$U_{inc} = e^{-jkr' \cos \psi} \quad (42)$$

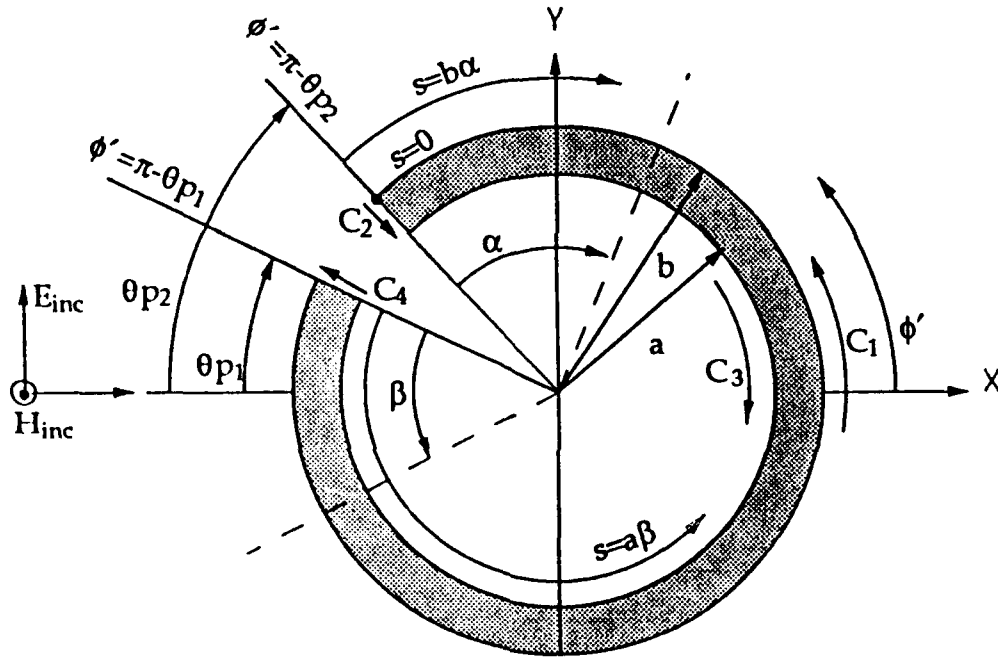


Fig.3 Circular slit cylinder

In Fig.3,  $\theta_{p1}$  and  $\theta_{p2}$  are the first and second slit angles from the  $-x$  axis respectively;  $b$  and  $a$  are the outer and inner radii of the cylinder respectively;  $s$  is the arc length and is taken as zero at  $\phi' = \pi - \theta_{p2}$  at the outer contour  $C_1$ ; the angles  $\alpha$  and  $\beta$  are considered zero at  $\phi' = \pi - \theta_{p2}$  and  $\phi' = \pi - \theta_{p1}$  respectively;  $s = b\alpha$  and  $s = a\beta$  are the arc lengths of the outer and inner surfaces respectively.

For the outer contour  $C_1$ , we get from fig.3,

$$U_S = \sum_{-\infty}^{\infty} A_n^{(b)} e^{jn\phi'} \Big|_{\phi' = \pi - \theta_{p_2} - \alpha} = \sum_{-\infty}^{\infty} A_n^{(b)} e^{jn(\pi - \theta_{p_2} - \alpha)} \quad (43)$$

$$\text{and } U_{Inc} = e^{-jkb\cos\phi'} \Big|_{\phi' = \pi - \theta_{p_2} - \alpha} = e^{-jkb\cos(\pi - \theta_{p_2} - \alpha)} \quad (44)$$

Similarly for the inner contour  $C_2$  we get

$$U_S = \sum_{-\infty}^{\infty} A_n^{(a)} e^{jn\phi'} \Big|_{\phi' = \beta + \pi - \theta_{p_1}} = \sum_{-\infty}^{\infty} A_n^{(a)} e^{jn(\pi + \beta - \theta_{p_1})} \quad (45)$$

$$\text{and } U_{Inc} = e^{-jka\cos\phi'} \Big|_{\phi' = \beta + \pi - \theta_{p_1}} = e^{-jka(\pi + \beta - \theta_{p_1})} \quad (46)$$

Therefore the current distribution for the outer and inner contours can be obtained by substituting (43) and (44) for the outer surface, and (45) and (46) for the inner surface respectively in (29). After simplification the following expression is obtained for the magnitude of the normalized surface currents.

For the outer contour  $C_1$ , we have

$$\left| \frac{J_\phi}{H_{Inc}} \right| = \left| - \left[ \sum_0^{\infty} \epsilon_n A_n^{(b)} (-1)^n \cos n(\alpha + \theta_{p_2}) + e^{jkb\cos(\theta_{p_2} + \alpha)} \right] \right|, \quad (47)$$

where  $\alpha$  varies from 0 to  $2\pi - \overline{\theta_{p_1} - \theta_{p_2}}$ ;  $C_1^{(b)}$  and  $C_2^{(b)}$  in  $A_n^{(b)}$  are given by the expressions from (16) as

$$C_1^{(b)} = + \frac{8k^2b^2 - 8jkb}{8k^2b^2 - 12jkb - 3} \quad \text{and} \quad C_2^{(b)} = - \frac{4}{8k^2b^2 - 12jkb - 3} \quad (48)$$

For the inner contour  $C_3$  we have

$$\left| \frac{J_\phi}{H_{inc}} \right| = \left| - \left[ \sum_0^{\infty} \epsilon_n A_n^{(a)} (-1)^n \cos n(\beta - \theta_{p1}) + e^{jk a \cos(\beta - \theta_{p1})} \right] \right|, \quad (49)$$

where  $\beta$  varies from 0 to  $2\pi - \overline{\theta_{p1} - \theta_{p2}}$ ;  $C_1^{(a)}$  and  $C_2^{(a)}$  are similar except that a negative sign is taken for  $C_1$  in (12) since the inner contour is a concave surface.

Along the linear portions  $C_2$  and  $C_4$ , we assume that the current varies linearly between the inner and outer curved surfaces.

#### B. DETERMINATION OF THE FAR FIELDS

From Fig.4 the total scattered magnetic field  $H_z^s$  for the hollow circular slit cylinder with finite thickness will be

$$H_z^s = H_{z_{c1}}^s + H_{z_{c2}}^s + H_{z_{c3}}^s + H_{z_{c4}}^s, \quad (50)$$

where  $C_1$  and  $C_3$  are the outer and inner contours with radii  $b$  and  $a$  respectively;  $\overline{\theta_{p1} - \theta_{p2}}$  is the total slit extent.

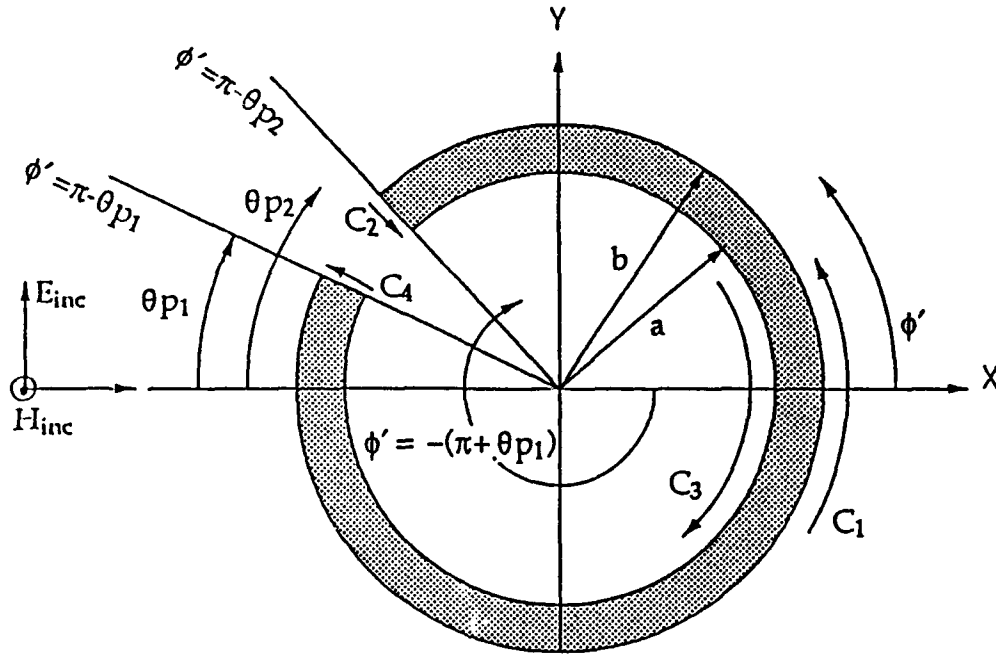


**Fig.4** slit cylinder geometry

From Fig.4 the integration limits in (50) would be

$$\int_C = \int_{C_1}^{r_o=b} + \int_{C_2}^{r_o=b-a} + \int_{C_3}^{r_o=a} + \int_{C_4}^{r_o=a-b} . \quad (51)$$

For the convex contour  $C_1$ , (38) is used with  $r_o=b$  and  $A_n = A_n^{(b)}$  where

$$A_n^{(b)} = \frac{C_1^{(b)} j^{-(n+1)} J_n'(kb)}{1 + C_2^{(b)} n^2} . \quad (52)$$

Substituting these values in (38) we get

$$\begin{aligned}
H_{z_{C_1}}^S = & -k \frac{e^{-jkr}}{\sqrt{r}} \frac{j}{4} \left( \frac{2j}{\pi k} \right)^{\frac{1}{2}} b \left[ \sum_{-\infty}^{\infty} j^{-n} J_n'(kb) \int_{C_1} e^{jkb \cos(\psi'-\phi)} \right. \\
& \left. \cdot e^{jn\phi'} d\phi' + \frac{1}{k} \sum_{-\infty}^{\infty} A_n^{(b)} \frac{\partial}{\partial r'} \Big|_{r'=b} \left( \int_{C_1} e^{jkr' \cos(\psi'-\phi)} e^{jn\phi'} d\phi' \right) \right]. \quad (53)
\end{aligned}$$

The integral over  $C_1$  is evaluated in the following fashion:

$$\begin{aligned}
& \int_{C_1} e^{jkb \cos(\psi'-\phi)} e^{jn\phi'} d\phi' \\
& = \int_0^{2\pi} e^{jkb \cos(\psi'-\phi)} e^{jn\phi'} - \int_{\pi-\theta_{p2}}^{\pi-\theta_{p1}} e^{jkb \cos(\psi'-\phi)} e^{jn\phi'} d\phi'. \quad (54)
\end{aligned}$$

The first integral can be evaluated in a closed form as in the previous chapter. In the second integral we let  $u = \pi - \phi' \Rightarrow d\phi' = -du$ . After some manipulation we get

$$\begin{aligned}
& \int_{C_1} e^{jkb \cos(\psi'-\phi)} e^{jn\phi'} d\phi' \\
& = (-1)^n [2\pi j^{-n} J_n'(kb) e^{jn\phi} - \int_{\theta_{p1}}^{\theta_{p2}} e^{-jkb \cos(u+\phi)} e^{-jn\phi} du]. \quad (55)
\end{aligned}$$

Substituting (55) in (53) and carrying out some manipulation we get

$$\begin{aligned}
H_{z_{c_1}}^S &= -k \frac{e^{-jkr}}{\sqrt{r}} \frac{j}{4} \left( \frac{2j}{\pi k} \right)^{\frac{1}{2}} b \left[ \sum_0^{\infty} 2\pi \epsilon_n [J_n'(kb) J_n(kb) + j^n A_n^{(b)} \right. \\
&\quad \cdot J_n'(kb) ] \cos n\phi - \sum_0^{\infty} \epsilon_n j^n J_n'(kb) \int_{\theta_{p1}}^{\theta_{p2}} e^{-jkb \cos(u+\phi)} \cos(nu) du \\
&\quad \left. + j \sum_0^{\infty} \epsilon_n A_n^{(b)} (-1)^n \int_{\theta_{p1}}^{\theta_{p2}} \cos(u+\phi) e^{-jkb \cos(u+\phi)} \cos(nu) du \right] . \quad (56)
\end{aligned}$$

For the inner contour  $C_3$  with radius  $a$ , which has a concave surface we have

$$\begin{aligned}
\frac{\partial H_z^S}{\partial v'} &= k \sum_{-\infty}^{\infty} j^{-n} J_n'(ka) e^{jn\phi'} , \\
H_z^S &= \sum_{-\infty}^{\infty} A_n(a) e^{jn\phi'} , \\
A_n^{(a)} &= \frac{C_1^{(a)} j^{-(n+1)} J_n'(ka)}{1 + C_2^{(a)} n^2} , \\
(\hat{r} \cdot \nabla') &= -\cos(\phi' - \phi) , \\
\text{and } \int_{C_3} ds' &= \int_{C_3} a d\phi' = -a \int_{C_1} d\phi' .
\end{aligned}$$

Substituting these values in (33) gives

$$\begin{aligned}
H_{z_{c_3}}^S &= -k \frac{e^{-jkr}}{\sqrt{r}} \frac{j}{4} \left( \frac{2j}{\pi k} \right)^{\frac{1}{2}} a \left[ \sum_{-\infty}^{\infty} j^{-n} J_n'(kr_0) \int_{C_3} e^{jkr_0 \cos(\phi' - \phi)} \right. \\
&\quad \left. \cdot e^{jn\phi'} d\phi' + \frac{1}{k} \sum_{-\infty}^{\infty} A_n \frac{\partial}{\partial r'} \Big|_{r'=a} \left( \int_{C_3} e^{jkr' \cos(\phi' - \phi)} e^{jn\phi'} d\phi' \right) \right] . \quad (57)
\end{aligned}$$

Following the same procedure as for the contour  $C_1$ , we can simplify the integral portion and after some manipulations we get

$$\begin{aligned}
H_{z_{C_3}}^S = & -k \frac{e^{-jkz}}{\sqrt{r}} \frac{j}{4} \left( \frac{2j}{\pi k} \right)^{\frac{1}{2}} a \left[ \sum_0^{\infty} 2\pi \epsilon_n [ (-1)^n J_n'(ka) J_n(ka) - j^{-n} A_n^{(a)} \right. \\
& \cdot J_n'(ka) ] \cos n\phi - \sum_0^{\infty} \epsilon_n j^n J_n'(ka) \int_{\theta_{p1}}^{\theta_{p2}} e^{-jk a \cos(u+\phi)} \cos(nu) du \\
& \left. + j \sum_0^{\infty} \epsilon_n A_n^{(a)} (-1)^n \int_{\theta_{p1}}^{\theta_{p2}} \cos(u+\phi) e^{-jk a \cos(u+\phi)} \cos(nu) du \right] . \quad (58)
\end{aligned}$$

For solving the linear portions  $C_2$  and  $C_4$ , we can ignore the edge effects since the OSRC approach does not currently provide edge current singularity behaviour as mentioned in ref. [1]. Therefore, for the linear portions we let  $U_s$  be equal to the average of  $U_s$  on the contours  $C_1$  and  $C_3$  at the position of the linear portion.

For contour  $C_2$  we have

$$U_s|_{C_2} = \frac{U_s|_{C_1} + U_s|_{C_3}}{2} \Big|_{\phi' = \pi - \theta_{p2}} = \sum_{-\infty}^{\infty} \left[ \frac{A_n^{(b)} + A_n^{(a)}}{2} \right] e^{jn\phi'} \Big|_{\phi' = \pi - \theta_{p2}} , \quad (59)$$

$$\frac{\partial H_z^S}{\partial v'} = \frac{\partial}{\partial r'} (e^{-jkr' \cos \phi'}) = -j k \cos(\pi - \theta_{p2}) e^{-jkr' \cos(\pi - \theta_{p2})} \quad (60)$$

$$\text{and} \quad (f \cdot \nu') = \cos(\phi' - \phi) = \cos(\pi - \theta_{p2} - \phi) . \quad (61)$$

Substituting these values in (33) and simplifying we get

$$\begin{aligned}
H_{z_{c_2}}^S = & \frac{e^{-jkr}}{\sqrt{I}} \frac{j}{4} \left( \frac{2j}{\pi k} \right)^{\frac{1}{2}} \left[ \frac{\cos \theta_{p_2}}{\cos \theta_{p_2} - \cos(\theta_{p_2} + \phi)} [e^{jka[\cos \theta_{p_2} - \cos(\theta_{p_2} + \phi)]} \right. \\
& \left. - e^{jkb[\cos \theta_{p_2} - \cos(\theta_{p_2} + \phi)]} \right] - \sum_{n=-\infty}^{\infty} \left[ \frac{A_n^{(b)} + A_n^{(a)}}{2} \right] \epsilon_n (-1)^n \cos n \theta_{p_2} \\
& \cdot [e^{-jka \cos(\theta_{p_2} + \phi)} - e^{-jkb \cos(\theta_{p_2} + \phi)}] . \quad (62)
\end{aligned}$$

Similarly for the linear portion  $C_4$  we have from Fig.4

$$U_S|_{C_4} = \frac{U_S|_{C_1} + U_S|_{C_3}}{2} |_{\phi' = \pi - \theta_{p_1}} = \sum_{n=-\infty}^{\infty} \left[ \frac{A_n^{(b)} + A_n^{(a)}}{2} \right] e^{jn\phi'} |_{\phi' = \pi - \theta_{p_1}} , \quad (63)$$

$$\frac{\partial H_z^S}{\partial \phi'} = -jkc \cos(\pi - \theta_{p_1}) e^{-jkr' \cos(\pi - \theta_{p_1})} \quad (64)$$

$$(f \cdot \phi') = \cos(\pi - \theta_{p_1} - \phi) . \quad (65)$$

Substituting values in (33) and after simplification we get

$$\begin{aligned}
H_{z_{c_4}}^S = & \frac{e^{-jkr}}{\sqrt{I}} \frac{j}{4} \left( \frac{2j}{\pi k} \right)^{\frac{1}{2}} \left[ \frac{\cos \theta_{p_1}}{\cos \theta_{p_1} - \cos(\theta_{p_1} + \phi)} [e^{jka[\cos \theta_{p_1} - \cos(\theta_{p_1} + \phi)]} \right. \\
& \left. - e^{jkb[\cos \theta_{p_1} - \cos(\theta_{p_1} + \phi)]} \right] - \sum_{n=-\infty}^{\infty} \left[ \frac{A_n^{(b)} + A_n^{(a)}}{2} \right] \epsilon_n (-1)^n \cos n \theta_{p_1} \\
& \cdot [e^{-jka \cos(\theta_{p_1} + \phi)} - e^{-jkb \cos(\theta_{p_1} + \phi)}] . \quad (66)
\end{aligned}$$

In summary, the total scattered magnetic field for the hollow circular slit cylinder is

$$\begin{aligned}
H_z^S = & \frac{e^{-jkx}}{\sqrt{r}} \frac{j}{4} \left( \frac{2j}{\pi k} \right)^{\frac{1}{2}} [-kb \left[ \sum_0^{\infty} 2\pi \epsilon_n [J_n(kb) J_n'(kb) \right. \\
& + j^n A_n^{(b)} J_n'(kb) ] \cos n\phi' - \sum_0^{\infty} \epsilon_n j^n J_n'(kb) \int_{\theta_{p1}}^{\theta_{p2}} e^{-jkb \cos(u+\phi)} \cos(nu) du \\
& + j \sum_0^{\infty} \epsilon_n A_n^{(b)} (-1)^n \int_{\theta_{p1}}^{\theta_{p2}} \cos(u+\phi) \cos(nu) e^{-jkb \cos(u+\phi)} du ] \\
& - ka \left[ \sum_0^{\infty} 2\pi \epsilon_n [ (-1)^n J_n(ka) J_n'(ka) - j^{-n} A_n^{(a)} J_n'(ka) ] \cos n\phi \right. \\
& - \sum_0^{\infty} \epsilon_n j^n J_n'(ka) \int_{\theta_{p1}}^{\theta_{p2}} e^{jka \cos(u+\phi)} \cos(nu) du \\
& + j \sum_0^{\infty} \epsilon_n A_n^{(a)} (-1)^n \int_{\theta_{p1}}^{\theta_{p2}} \cos(u+\phi) e^{jka \cos(u+\phi)} \cos(nu) du ] \\
& - \left[ \frac{\cos \theta_{p2}}{\cos \theta_{p2} - \cos(\theta_{p2} + \phi)} [ e^{jka[\cos \theta_{p2} - \cos(\theta_{p2} + \phi)]} - e^{jkb[\cos \theta_{p2} - \cos(\theta_{p2} + \phi)]} ] \right. \\
& - \sum_0^{\infty} \epsilon_n (-1)^n \left[ \frac{A_n^{(b)} + A_n^{(a)}}{2} \right] \cos n\theta_{p2} [ e^{-jka \cos(\theta_{p2} + \phi)} - e^{-jkb \cos(\theta_{p2} + \phi)} ] ] \\
& - \left[ \frac{\cos \theta_{p1}}{\cos \theta_{p1} - \cos(\theta_{p1} + \phi)} [ e^{jka[\cos \theta_{p1} - \cos(\theta_{p1} + \phi)]} - e^{jkb[\cos \theta_{p1} - \cos(\theta_{p1} + \phi)]} ] \right. \\
& \left. - \sum_0^{\infty} (-1)^n \left[ \frac{A_n^{(b)} + A_n^{(a)}}{2} \right] \cos n\theta_{p1} [ e^{-jka \cos(\theta_{p1} + \phi)} - e^{-jkb \cos(\theta_{p1} + \phi)} ] ] \right] \quad (67)
\end{aligned}$$

The scattering width  $\sigma_{2-D}$  is defined as (ref.[6])

$$\sigma_{2-D} = 2\pi r \frac{|H_z^S|^2}{|H_z^{inc}|^2} \quad (68)$$

For the scattered field given in (49) we have

$$\begin{aligned}
\sigma_{2-D} = & \frac{1}{4k} \left| -kb \left[ \sum_0^{\infty} 2\pi \epsilon_n \left[ J_n(kb) J_n'(kb) + j A_n^{(b)} J_n'(kb) \right] \cos n\phi' \right. \right. \\
& - \sum_0^{\infty} \epsilon_n j^n J_n'(kb) \int_{\theta_{p1}}^{\theta_{p2}} e^{-jkbcos(u+\phi)} \cos(nu) du \\
& + j \sum_0^{\infty} \epsilon_n A_n^{(b)} (-1)^n \int_{\theta_{p1}}^{\theta_{p2}} \cos(u+\phi) \cos(nu) e^{-jkbcos(u+\phi)} du \left. \right] \\
& - ka \left[ \sum_0^{\infty} 2\pi \epsilon_n \left[ (-1)^n J_n(ka) J_n'(ka) - j A_n^{(a)} J_n'(ka) \right] \cos n\phi \right. \\
& - \sum_0^{\infty} \epsilon_n j^n J_n'(ka) \int_{\theta_{p1}}^{\theta_{p2}} e^{jkacos(u+\phi)} \cos(nu) du \\
& + j \sum_0^{\infty} \epsilon_n A_n^{(a)} (-1)^n \int_{\theta_{p1}}^{\theta_{p2}} \cos(u+\phi) e^{jkacos(u+\phi)} \cos(nu) du \left. \right] \\
& - \left[ \frac{\cos\theta_{p2}}{\cos\theta_{p2} - \cos(\theta_{p2}+\phi)} \left[ e^{jka[\cos\theta_{p2} - \cos(\theta_{p2}+\phi)]} - e^{jkb[\cos\theta_{p2} - \cos(\theta_{p2}+\phi)]} \right] \right. \\
& - \sum_0^{\infty} \epsilon_n (-1)^n \left[ \frac{A_n^{(b)} + A_n^{(a)}}{2} \right] \cos n\theta_{p2} \left[ e^{-jkacos(\theta_{p2}+\phi)} - e^{-jkbcos(\theta_{p2}+\phi)} \right] \left. \right] \\
& - \left[ \frac{\cos\theta_{p1}}{\cos\theta_{p1} - \cos(\theta_{p1}+\phi)} \left[ e^{jka[\cos\theta_{p1} - \cos(\theta_{p1}+\phi)]} - e^{jkb[\cos\theta_{p1} - \cos(\theta_{p1}+\phi)]} \right] \right. \\
& - \sum_0^{\infty} (-1)^n \left[ \frac{A_n^{(b)} + A_n^{(a)}}{2} \right] \cos n\theta_{p1} \left[ e^{-jkacos(\theta_{p1}+\phi)} - e^{-jkbcos(\theta_{p1}+\phi)} \right] \left. \right] \Big|^2 \quad (69)
\end{aligned}$$

#### IV. NUMERICAL RESULTS AND DISCUSSION

All analyses were carried out for the TE polarization case and when the incident wave is incident from the  $-x$  axis, i.e. from  $\phi=180^\circ$ . In all cases  $a$  and  $b$  denote the inner and outer radii of the cylinders.

For the circular cylinder, Figs. 5 and 6 show the comparisons of the normalized surface current distribution between the present formulation (32) and of ref.[1], both using the OSRC approach for  $kb=5$  and  $10$  respectively. The results are comparable, checking the validity of our formulation. It was shown in ref.[1], that the results approach the exact solution. The computer program to compute the normalized surface current distribution using the OSRC approach is given in Appendix A. Figs. 7,8 and 9 show the comparisons of the bistatic widths for the circular cylinder between the present formulation and ref.[8] for  $kb=1,5$  and  $10$  respectively. Ref.[8] uses the rigorous moment method technique for determining the scattering cross sections of infinite cylinders of arbitrary geometrical cross section. The results again are in good agreement. The computer program to compute the scattering width for circular cylinders using the OSRC approach is given in Appendix B. Figs.10 and 11 show the comparisons of forward ( $\phi=0^\circ$ ) and backward ( $\phi=180^\circ$ ) scattering

widths respectively, versus  $kb$ , between the computed and ref.[5] (exact solution). It is seen that the results due to the OSRC approach show some deviation at higher frequencies (i.e. for large  $kb$ ) in both cases. The computer program to compute  $\sigma/\pi b$  versus  $kb$  is given in Appendix C.

For the hollow circular slit cylinder, Fig.12 shows the comparison of the normalized surface current distribution for a hollow semi-circular cylinder obtained using the present formulation (47) and (49) and that in ref.[7]. The problem of scattering in ref.[7] is solved by means of an integral equation. In Fig.14, the current density, normalized to unity for the magnetic field strength of the incident wave, is plotted versus perimeter  $s$  normalized to unity for the half perimeter. The distance variable  $s$  is taken equal to zero at the point on the center face nearest the source of the incident wave. Moving clockwise around the perimeter,  $s$  increases in value reaching the value  $s=1$  at the center face furthest from the source. The results again are comparable to the exact solution. The computer program to compute (47) and (49) for the circular slit cylinder is given at Appendix D. Fig.13 shows the comparison of the scattering width. The results obtained using the OSRC approach are quite different from the exact solutions as shown in Fig.13. This is in spite of the good agreement in the magnitude of the current distribution. At this point it seemed necessary to carry out some phase comparisons for the current distribution, however

no known results were available. The computer program in Appendix E was thoroughly checked for any bugs and even tested for circular cylinders which yielded satisfactory results. It is felt that the disagreement in the scattering width due to the OSRC method is probably due to the incorrect modeling of phase of the current distribution. The OSRC technique assumes waves of only one kind (outgoing) to exist on the scattering surfaces which may not yield correct results for concave structures.

Fig.14 shows comparisons of forward scattering width ( $\phi=0^\circ$ ) for the hollow circular slit cylinder ( $b=a$  and total slit angle of  $10^\circ$ ) between the OSRC approach and the full circular cylinder from ref.[5] (exact solution). Fig.15 shows the comparison between the OSRC approach and ref.[5] results for the hollow circular slit cylinder. Such shapes are expected to have cross section resonances, indicating that there is interior information contained in the exterior scattering data. Here, again the results are quite different. Another peculiar result was that we were getting the same results for forward and backward scattering widths using the computer program given in Appendix F. This might be due to some unforeseen error in the program.

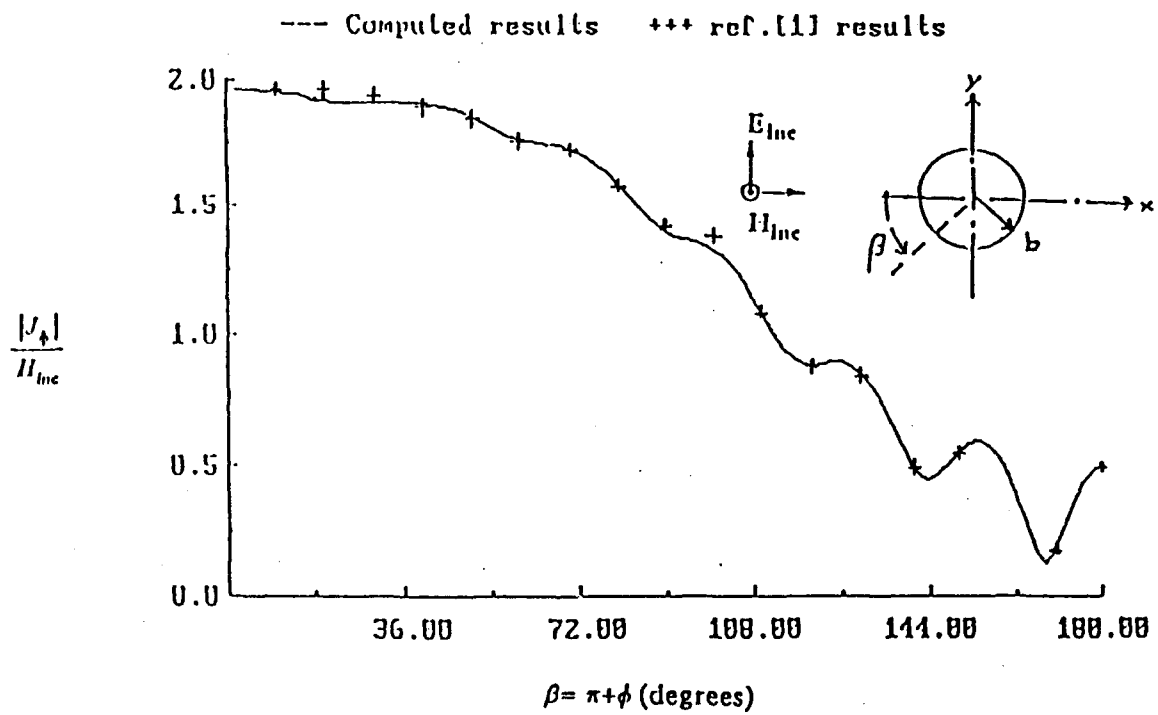


Fig.5 Comparison of surface current distribution on a PEC circular cylinder with  $kb=5$ .

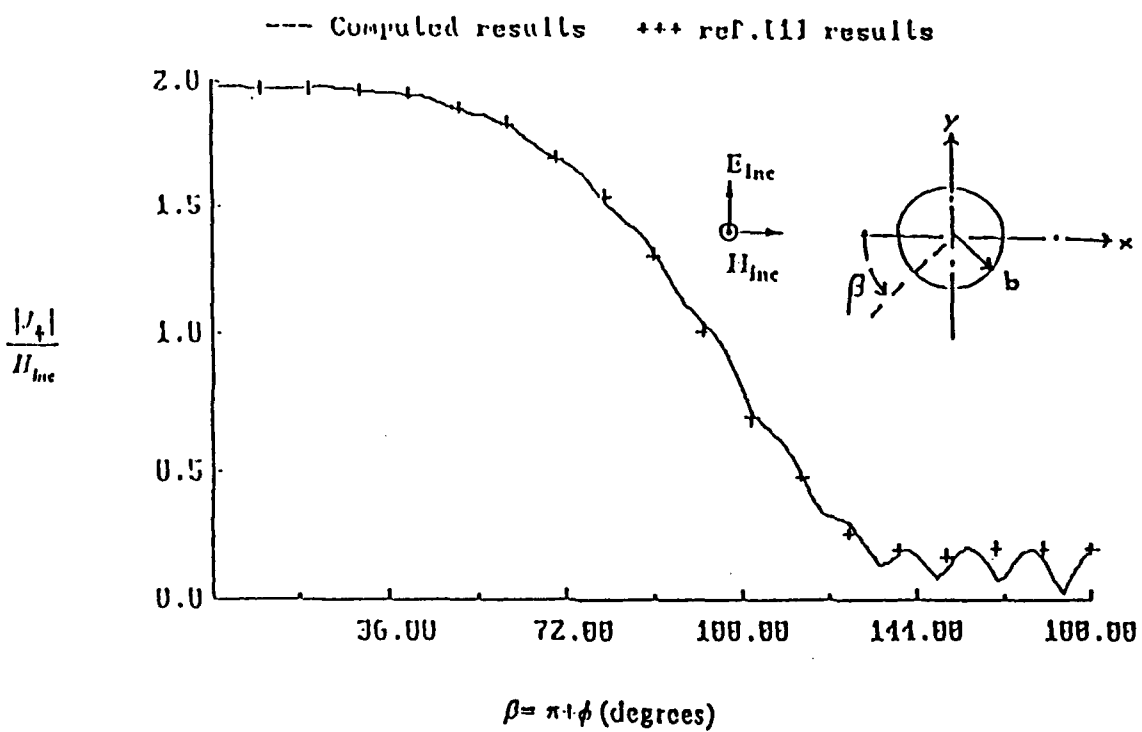


Fig.6 Comparison of surface current distribution on a PEC cylinder with  $kb=10$

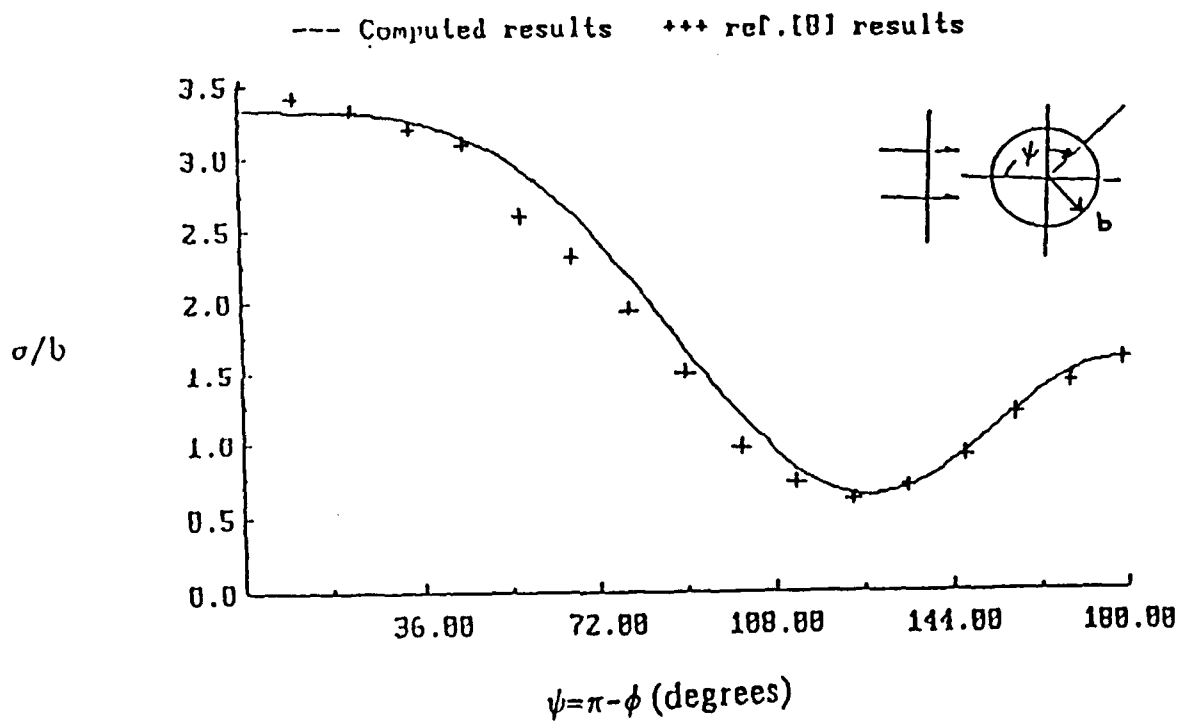
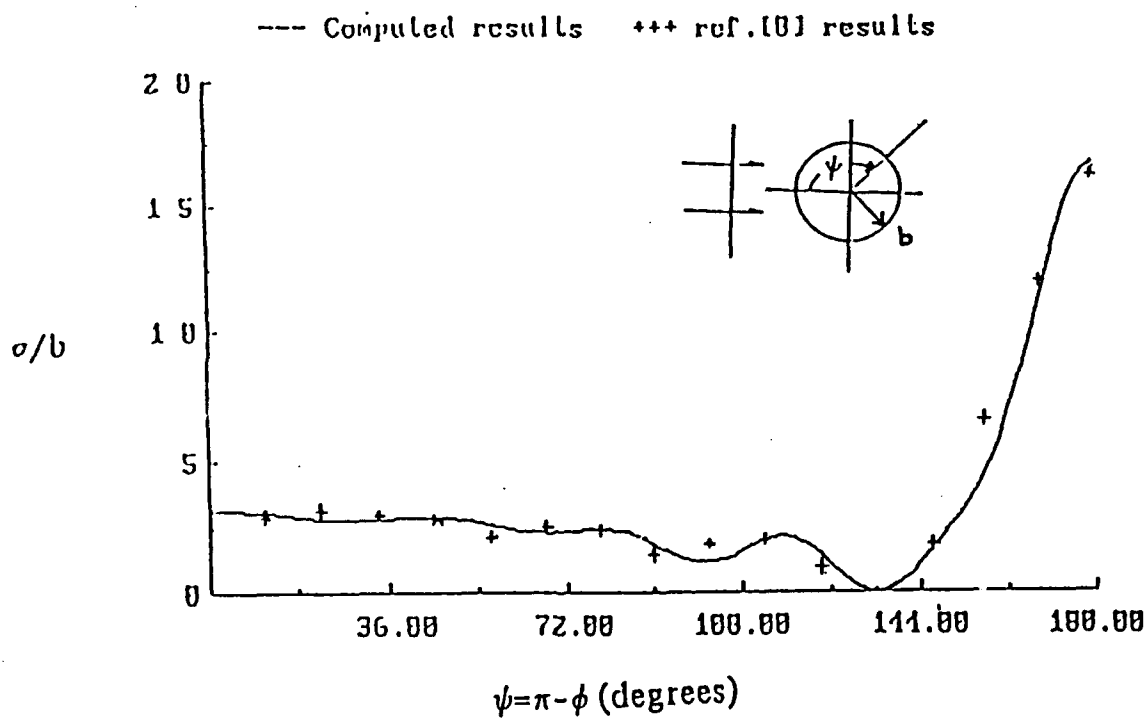


Fig.7 Comparison of bistatic scattering width for the circular cylinder with  $kb=1$ .



**Fig.8 Comparison of bistatic scattering width for the circular cylinder with  $kb=5$ .**

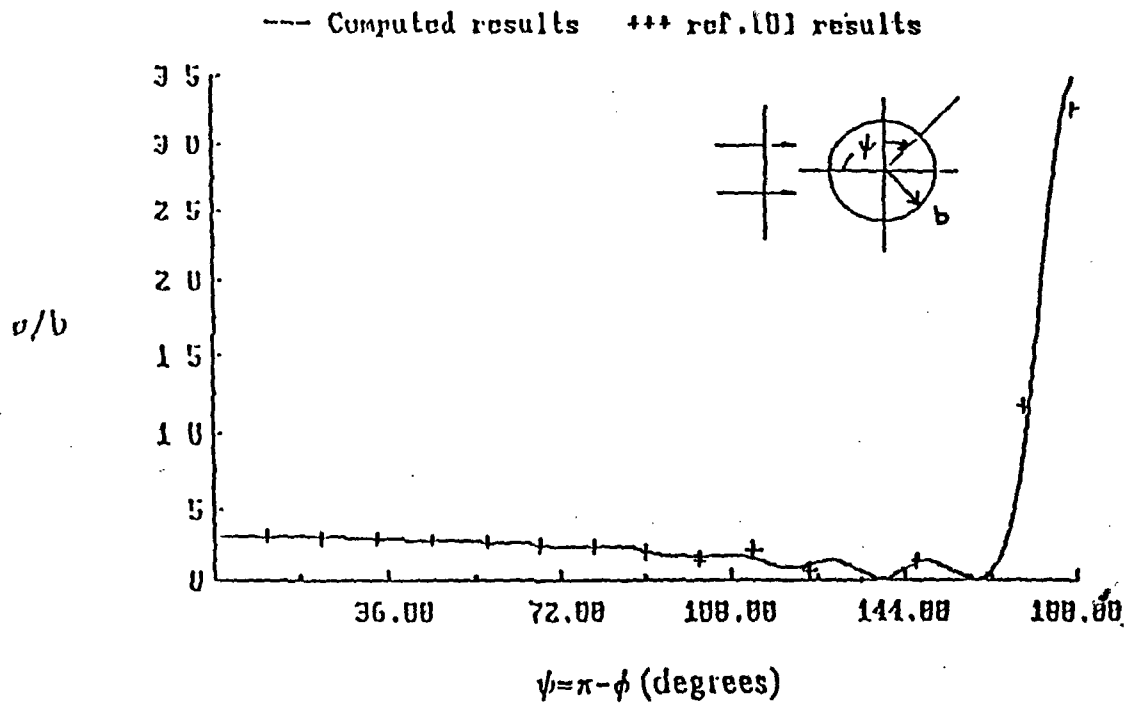


Fig.9 - Comparison of bistatic scattering width for the circular cylinder with  $kb=10$ .

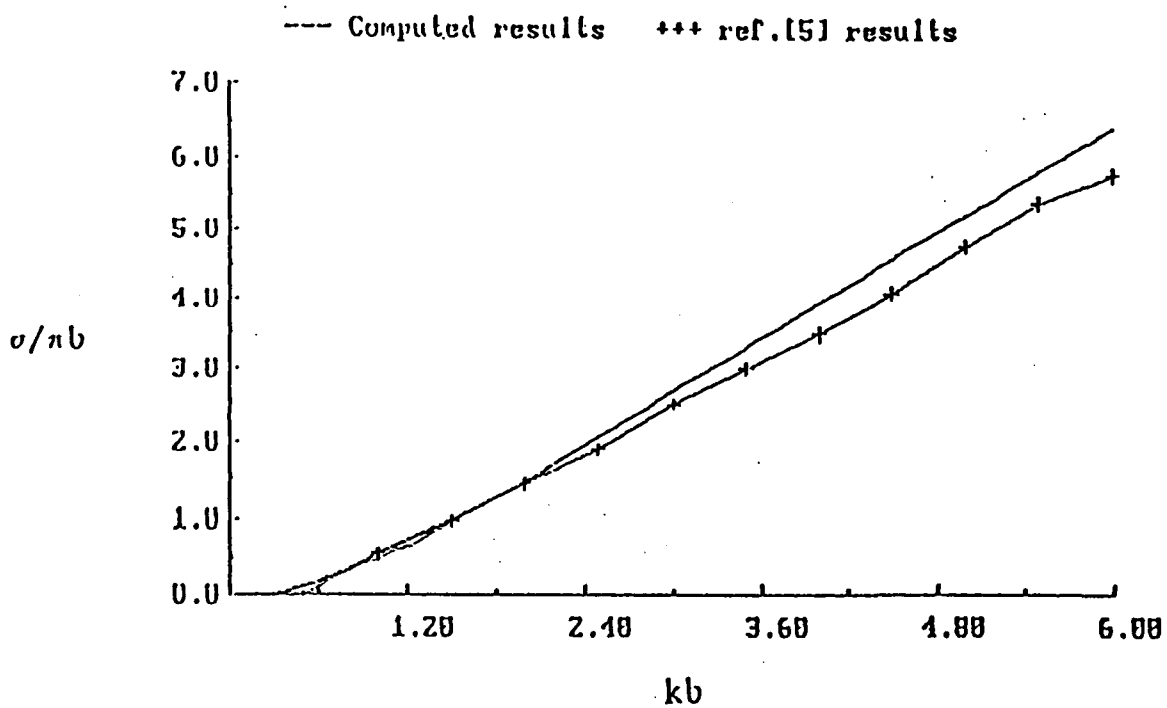


Fig.10 Comparison of forward scattering width ( $\phi=0^\circ$ ) for the circular cylinder between the computed (OSRC approach) and ref.[5] (exact solution).

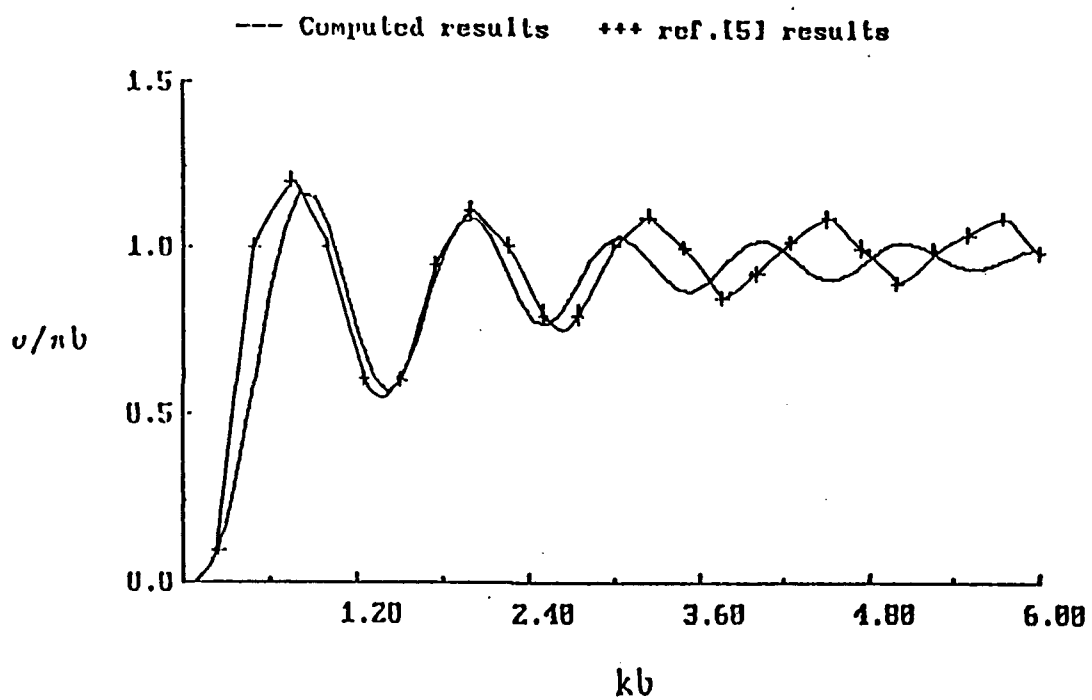


Fig.11 Comparison of backward scattering width ( $\phi=180^\circ$ ) for the circular cylinder between the computed (OSRC approach) and ref.[5] (exact solution).

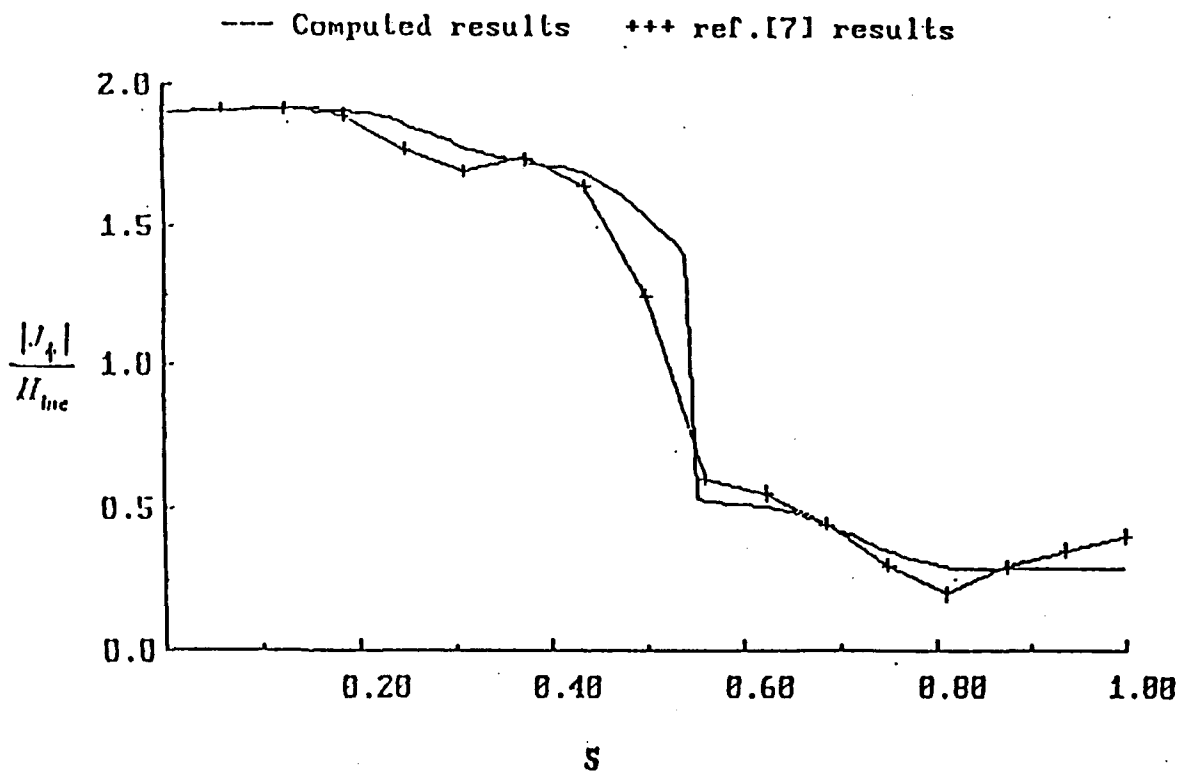
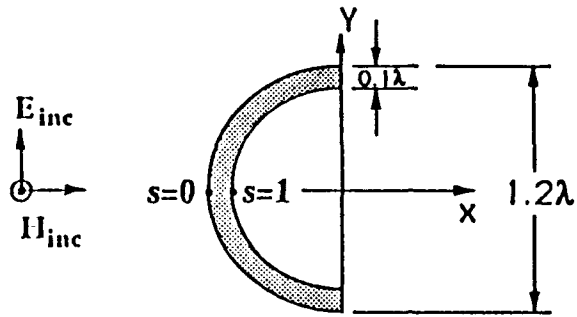


Fig.12 Comparison of surface current distribution for the hollow semi-circular slit cylinder ( $J_s$  versus  $s$ ).

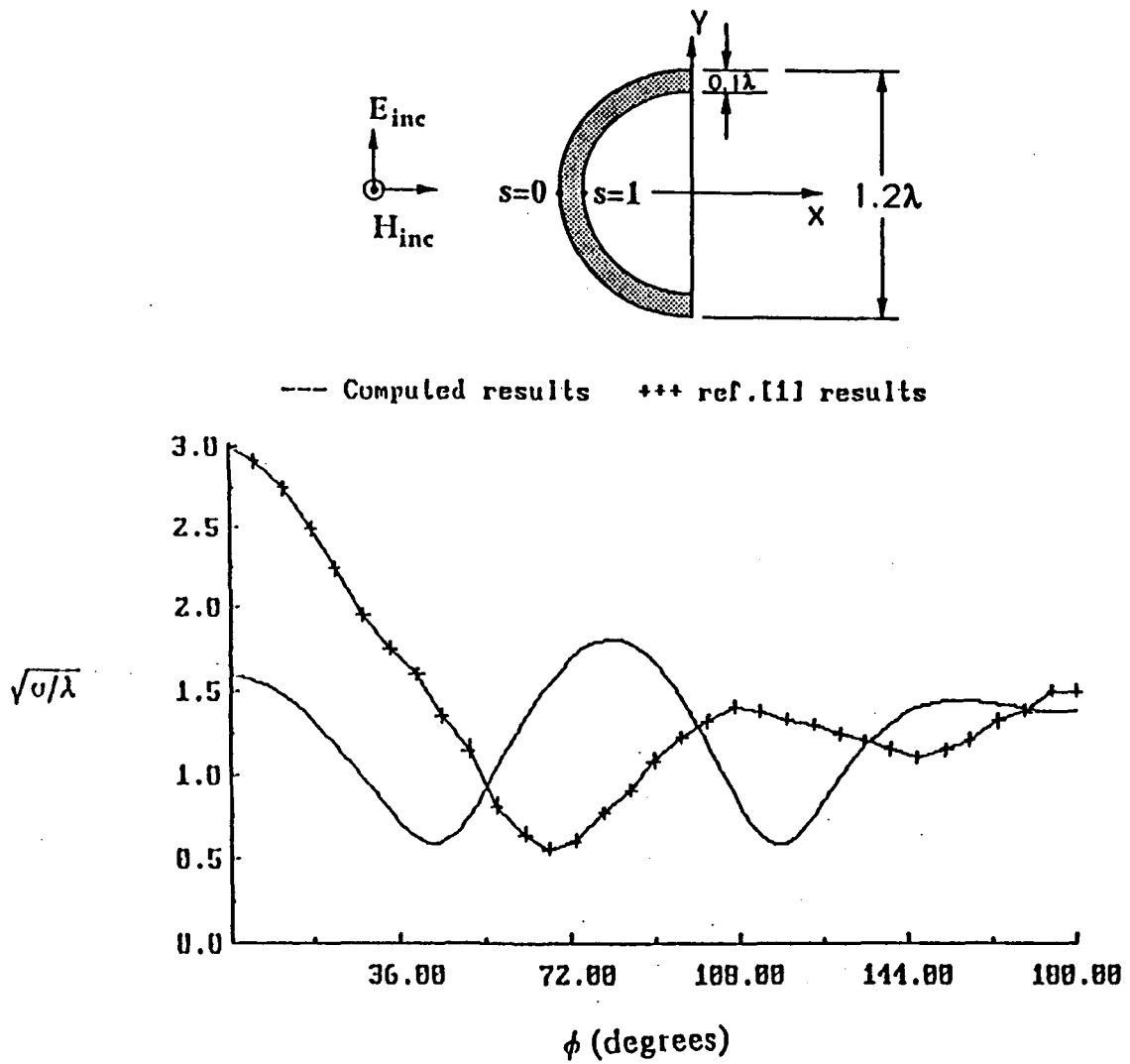


Fig.13 Comparison of scattering width for the hollow semi-circular slit cylinder.

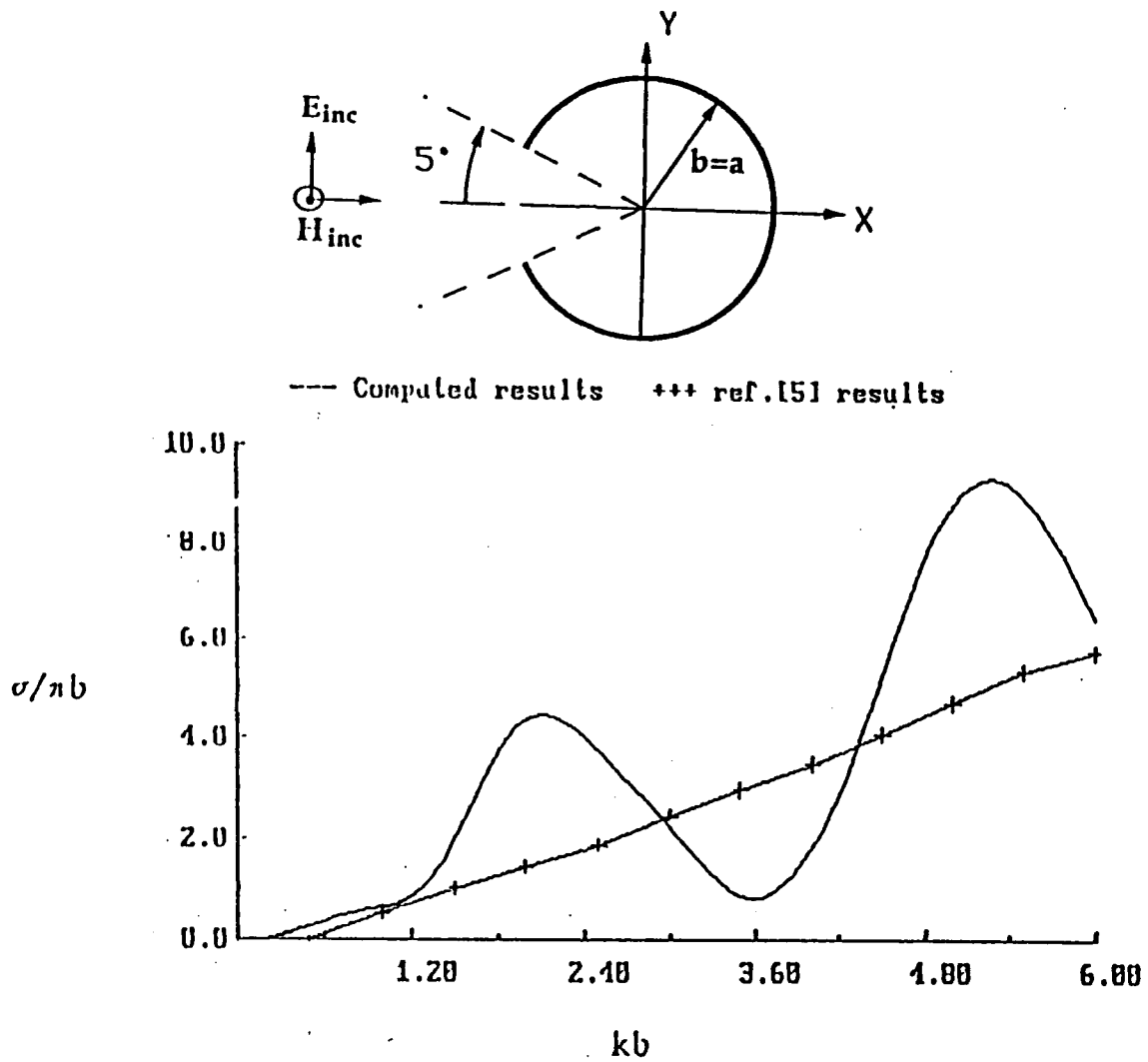


Fig.14 Comparison of forward scattering width for a hollow circular slit cylinder with  $b=a$  and total slit angle of  $10^\circ$  and full circular cylinder from ref.[5] .

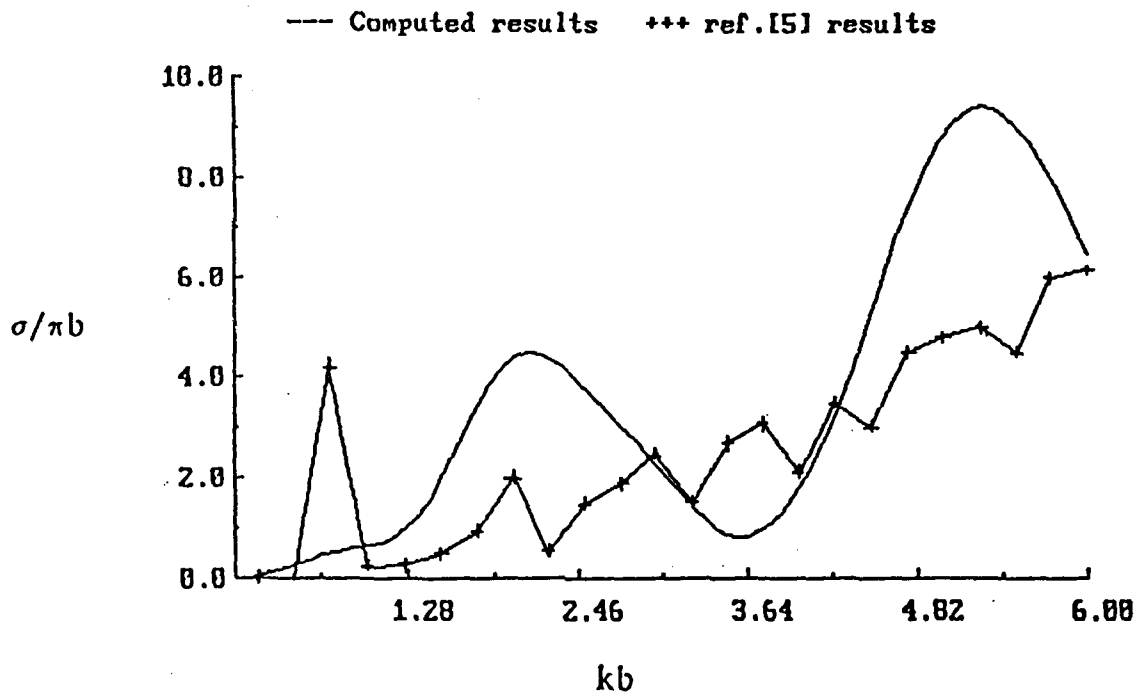
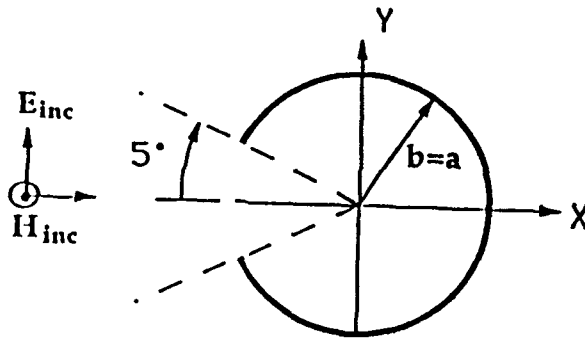


Fig.15 Comparison of forward scattering width for the hollow circular slit cylinder with  $b=a$  and slit angle of  $10^\circ$ .

## V. CONCLUSIONS

The OSRC approach was applied to circular and hollow slit circular cylinders. For circular cylinders the normalized surface current distribution agrees very well with the exact solution. Scattering width results, with different values of  $kb$  were also comparable with the exact solution, as long as  $kb$  was not large. For the case of hollow circular slit cylinders, the OSRC normalized surface current distribution was comparable to exact solution results. However, in case of the scattering width, the slit cylinder results were quite different from the exact solution. This indicated a need to carry out phase comparisons of the OSRC surface current distribution with the exact solution.

It is possible that the OSRC approach may not be applicable to concave structures and also for higher values of  $kb$  for convex bodies. As mentioned earlier, both outward and inward travelling waves can exist in the interior region of the concave scatterer. Since the OSRC approach assumes waves of only one kind, it is not expected to be applicable to concave bodies. Further the method fails when the scattering surface has cavity shaped objects.

**APPENDIX A. COMPUTER PROGRAM TO COMPUTE CURRENT DISTRIBUTION FOR CIRCULAR CYLINDERS**

```

C      THIS PROGRAM COMPUTES THE SURFACE CURRENT DISTRIBUTION FOR A
C      CIRCULAR CYLINDER FOR TRANSVERSE ELECTRIC CASE USING OSRC
C      APPROACH.
      REAL*8 J(0:200),Y(0:200),DY(0:200),DJ(0:200),K1D,K2D
      REAL*8 J1(0:200),Y1(0:200),DY1(0:200),DJ1(0:200)
      REAL EN,NMX,P,PHI,K,K1,DTR,PI,FR,B,JPHI
      INTEGER NMAX,N
      COMPLEX CB1,CB2,i,S1,S2,S3,S4,DN(999),JP
      OPEN(3,FILE='DAT.1')
      WRITE(*,*) 'ENTER THE WAVE NUMBER K (REAL) IN 1/METERS'
      READ(*,*) K
      WRITE(*,*) 'ENTER THE RADIUS (REAL) IN METERS'
      READ(*,*) B
      WRITE(*,*) 'ENTER NMAX (INT)'
      READ(*,*) NMAX
      PI=3.1415927
      DTR=PI/180.
      i=(0,1)
      K1=K*B
      K1D=DBLE(K1)
      CB1=(8.*K1**2-8.*i*K1)/(8.*K1**2-12.*i*K1-3.)
      CB2=-4./(8.*K1**2-12.*i*K1-3.)
      CALL BES(NMAX,K1D,J,Y,DJ,DY)
C PLOTTING ROUTINE
      WRITE(3,100) 'SURFACE CURRENT DISTRIBUTION FOR CIRCULAR CYL.'
      NPHI=91
      PHI1=0.
      PHI2=180.
      WRITE(3,110) NPHI
      WRITE(3,120) PHI1
      WRITE(3,120) PHI2
      DO 33 P=0.,180.,2.
        PHI=DTR*P
        S4=(0,0)
        DO 22 N=1,NMAX+1
          NMX=FLOAT(N)-1.
          IF(NMX.EQ.0.) THEN
            EN=1.
          ELSE
            EN=2.
          ENDIF
          S1=(0,0)
          S2=(0,0)
          S3=(0,0)
          S1=CB1*i**(-1) * DJ(NMX)/(1.+CB2*NMX**2)
          S2=J(NMX)
          S3=COS(NMX*(PI+PHI))
          DN(N)=- (EN*i**(-NMX) *(S1+S2) *S3)
        
```

```
      S4=S4+DN(N)
22    CONTINUE
      JP=S4
      JPHI=CABS(JP)
      WRITE(3,120) JPHI
33    CONTINUE
      CLOSE(3)
100   FORMAT(A)
110   FORMAT(I5)
120   FORMAT(E12.3)
      STOP
      END
```

APPENDIX B. COMPUTER PROGRAM TO COMPUTE  $\sigma/b$  FOR CIRCULAR CYLINDERS

```

C      THIS PROGRAM COMPUTES THE SCATTERING WIDTH FOR A CIRCULAR
C      CYLINDER FOR THE TRANSVERSE ELECTRIC POLARIZATION CASE
C      USING THE ON - SURFACE RADIATION CONDITION APPROACH.
C      ANGLE SI = PI - PHI GOING CLOCKWISE FROM -180 DEGREES
C      ALONG THE X-AXIS.
      REAL*8 J(0:200),Y(0:200),DY(0:200),DJ(0:200),K1D
      INTEGER N,NMAX
      REAL TA,TB,K,K1,K2,TP1,TP2,FILON,FR,B,A,L,PI,P,NMX,EN,PHI
      COMPLEX DN(999),S2,S3,S4,CN1,i,CB1,CB2
      OPEN(3,FILE='DAT.2')
      WRITE(*,*) 'ENTER THE WAVE NUMBER(REAL) IN 1/METERS'
      READ(*,*) K
      WRITE(*,*) 'ENTER THE OUTER RADIUS(REAL) IN METERS'
      READ(*,*) B
      WRITE(*,*) 'ENTER NMAX(INTEGER)'
      READ(*,*) NMAX
      PI=3.1415927
      DTR=PI/180.
      i=(0,1)
      K1=K*B
      K1D=DBLE(K1)
      CB1=(8.*K1**2-8.*i*K1)/(8.*K1**2-12.*i*K1-3.)
      CB2=-4./(8.*K1**2-12.*i*K1-3.)
      CALL BES(NMAX,K1D,J,Y,DJ,DY)
C      PLOTTING ROUTINE
      WRITE(3,960)'TE CASE PEC CIR. CYLINDER SCATTERING WIDTH '
      NPHI=91
      PHI1=0.
      PHI2=180.
      WRITE(3,970) NPHI
      WRITE(3,980) PHI1
      WRITE(3,980) PHI2
      DO 50 P =0.,180.,2.
          PHI=DTR*P
C      EVALUATING THE FUNCTION CN1
          S2=(0,0)
          DO 800 N=1,NMAX+1
              NMX=FLOAT(N)-1.
              S3=(0,0)
              S4=(0,0)
              IF(NMX.EQ.0.) THEN
                  EN=1.
              ELSE
                  EN=2.
              ENDIF
              S3=J(NMX)*DJ(NMX)
              S4=i**(-1)*CB1*DJ(NMX)**2/(1+CB2*NMX**2)
              DN(N)=2.*PI*EN*(S3+S4)*COS(NMX*(PI-PHI))
              S2=S2+DN(N)

```

```
800      CONTINUE
          CN1=S2
C  EVALUATING THE SCATTERING WIDTH DIVIDED BY CYLINDER RADIUS B
          SIGMA=1./(4.*K1)*CABS(-K1*CN1)**2
          WRITE(3,980) SIGMA
50      CONTINUE
          CLOSE(3)
960     FORMAT(A)
970     FORMAT(I5)
980     FORMAT(E12.3)
STOP
END
```

APPENDIX C. COMPUTER PROGRAM TO COMPUTE  $\sigma/\pi b$  versus kb FOR CIRCULAR CYLINDERS

```

C      THIS PROGRAM COMPUTES THE SCATTERING WIDTH FOR A CIRCULAR
C      CYLINDER FOR THE TRANSVERSE ELECTRIC POLARIZATION CASE
C      USING THE ON - SURFACE RADIATION CONDITION APPROACH.
C      (SIGMA /PI*B Vs KB)
      REAL*8 J(0:200),Y(0:200),DY(0:200),DJ(0:200),K1D
      INTEGER N,NMAX
      REAL TA,TB,K,K1,K2,TP1,TP2,FILON,FR,B,A,L,PI,P,NMX,EN,PHI,R
      COMPLEX DN(999),S2,S3,S4,CN1,i,CB1,CB2
      OPEN(3,FILE='DAT.3')
      WRITE(*,*) 'ENTER THE PHI ANGLE(REAL) IN DEGREES'
      READ(*,*) P
      WRITE(*,*) 'ENTER THE OUTER RADIUS(REAL) IN METERS'
      READ(*,*) B
      WRITE(*,*) 'ENTER NMAX(INTEGER)'
      READ(*,*) NMAX
      PI=3.1415927
      DTR=PI/180.
      PHI = DTR*P
      i=(0,1)
C      PLOTTING ROUTINE
      WRITE(3,960) 'TE CASE PEC CIR. CYLINDER SCATTERING WIDTH '
      NPHI=59
      PHI1=0.1
      PHI2=6.
      WRITE(3,970) NPHI
      WRITE(3,980) PHI1
      WRITE(3,980) PHI2
      DO 50 R =0.1,6.,.1
          K1=R*B
          K1D=DBLE(K1)
          CB1=(8.*K1**2-8.*i*K1)/(8.*K1**2-12.*i*K1-3.)
          CB2=-4./(8.*K1**2-12.*i*K1-3.)
          CALL BES(NMAX,K1D,J,Y,DJ,DY)
C      EVALUATING THE FUNCTION CN1
          S2=(0,0)
          DO 800 N=1,NMAX+1
              NMX=FLOAT(N)-1.
              S3=(0,0)
              S4=(0,0)
              IF(NMX.EQ.0.) THEN
                  EN=1.
              ELSE
                  EN=2.
              ENDIF
              S3=J(NMX)*DJ(NMX)
              S4=i**(-1.)*CB1*DJ(NMX)**2/(1.+CB2*NMX**2)
              DN(N)=2.*PI*EN*(S3+S4)*COS(NMX*PHI)
              S2=S2+DN(N)
800      CONTINUE

```

```
          CN1=S2
C  EVALUATING THE SCATTERING WIDTH DIVIDED BY CYLINDER RADIUS B
      SIGMA=1./(4.*K1*PI)*CABS(-K1*CN1)**2
      WRITE(3,980) SIGMA
50     CONTINUE
      CLOSE(3)
960    FORMAT(A)
970    FORMAT(I5)
980    FORMAT(E12.3)
      STOP
      END
```

APPENDIX D. COMPUTER PROGRAM TO COMPUTE  $J_c$  FOR SLIT CIRCULAR CYLINDERS

C THIS PROGRAM COMPUTES THE SURFACE CURRENT DISTRIBUTION FOR A  
C CIRCULAR SLIT CYLINDER FOR TRANSVERSE ELECTRIC CASE USING OSRC  
C APPROACH.

```

REAL*8 J(0:200),Y(0:200),DJ(0:200),DY(0:200),K1D,K2D
REAL*8 J1(0:200),Y1(0:200),DJ1(0:200),DY1(0:200)
REAL EN,NMX,P,PHI,K,K1,K2,SMAX,PI,FR,A,B,JPHI,L,S,S2,SM2,R
REAL SMAX2
INTEGER NMAX,N
COMPLEX CB1,CB2,CA1,CA2,i,S1,S3,S4,DN(999),JP,S5
OPEN(3,FILE='DAT.5')
WRITE(*,*) 'ENTER THE FREQUENCY (REAL) IN MHZ'
READ(*,*) FR
WRITE(*,*) 'ENTER THE FIRST SLIT ANGLE (REAL) IN DEGREES'
READ(*,*) TA
WRITE(*,*) 'ENTER THE SECOND SLIT ANGLE (REAL) IN DEGREES'
READ(*,*) TB
WRITE(*,*) 'ENTER NMAX (INT)'
READ(*,*) NMAX
PI=3.1415927
i=(0,1)
DTR=PI/180.
K=PI*FR/150.
L=300./FR
B=.6*L
A=.5*L
K1=K*B
K2=K*A
K1D=DBLE(K1)
K2D=DBLE(K2)
CALL BES(NMAX,K1D,J,Y,DJ,DY)
CALL BES(NMAX,K2D,J1,Y1,DJ1,DY1)
TP1=TA/57.29578
TP2=TB/57.29578
CB1=(8.*K1**2-8.*i*K1)/(8.*K1**2-12.*i*K1-3.)
CB2=-4./(8.*K1**2-12.*i*K1-3.)
CA1=-(8.*K2**2-8.*i*K2)/(8.*K2**2-12.*i*K2-3.)
CA2=-4./(8.*K2**2-12.*i*K2-3.)
C PLOTTING ROUTINE
WRITE(3,100) ' CURRENT DISTRIBUTION FOR CIRCULAR SLIT CYL.'
NPHI=95
PHI1=0.
PHI2=1.
WRITE(3,110) NPHI
WRITE(3,120) PHI1
WRITE(3,120) PHI2
SMAX=B*(2*PI-ABS(TP2-TP1)-PI/2)+(B-A)+A*(2*PI-ABS(TP2-TP1)-PI/2)
DO 33 P=0.,.52,.01
    S=P*SMAX/B+PI/2

```

```

S3=EXP(i*K1*COS(TP2+S))
S4=(0,0)
DO 22 N=1,NMAX+1
  NMX=FLOAT(N)-1.
  IF(NMX.EQ.0.) THEN
    EN=1.
  ELSE
    EN=2.
  ENDIF
  S1=(0,0)
  S2=0.
  S1=EN*CB1*i**(NMX-1.) * DJ(NMX)/(1.+CB2*NMX**2)
  S2=COS(NMX*(S+TP2))
  DN(N)=S1*S2
  S4=S4+DN(N)
22  CONTINUE
  JP=-(S4+S3)
  JPHI=CABS(JP)
  WRITE(3,120) JPHI
33  CONTINUE
C PLOTTING ROUTINE

      DO 10 R=.57,1.,.01
        S= (R-.57)*SMAX/A
S5=EXP(i*K2*COS(TP1-S))
S4=(0,0)
DO 5 N=1,NMAX+1
  NMX=FLOAT(N)-1.
  IF(NMX.EQ.0.) THEN
    EN=1.
  ELSE
    EN=2.
  ENDIF
  S1=(0,0)
  S2=0.
S1=EN*CA1*i**(NMX-1.)*DJ1(NMX)/(1.+CA2*NMX**2)
S2=COS(NMX*(TP1-S))
DN(N)=S1*S2
S4=S4+DN(N)
5  CONTINUE
JP=-(S4+S5)
JPHI=CABS(JP)
WRITE(3,120) JPHI
10  CONTINUE
CLOSE(3)
100  FORMAT(A)
110  FORMAT(I5)
120  FORMAT(E12.3)
      STOP
      END

```

**APPENDIX E. COMPUTER PROGRAM FOR  $\sqrt{\sigma/\lambda}$  versus  $\phi$  FOR SLIT CIRCULAR CYLINDERS**

C THIS PROGRAM COMPUTES THE SCATTERING WIDTH  $\sqrt{\sigma/\lambda}$  FOR A CIRCULAR HOLLOW CYLINDER WITH A SLIT OF ANY SIZE FOR THE TRANSVERSE ELECTRIC POLARIZATION CASE USING THE ON - SURFACE RADIATION CONDITION APPROACH.

```

REAL*8 J(0:200),Y(0:200),DY(0:200),DJ(0:200),K1D,K2D
REAL*8 J1(0:200),Y1(0:200),DJ1(0:200),DY1(0:200),H1
REAL EN,NMX,R,U,UU,H,P,PI,PHI,FAC,F(99),P1
INTEGER M,N,NT,NN,NMAX
REAL TA,TB,K,K1,K2,TP1,TP2,FILON,FR,B,A,L
COMPLEX P2,P3,i,S1,T1,T2,T3,T4,CB1,CB2,CA1,CA2
COMPLEX C1,C2,C3,C4,C5,C6,C7,C8,CN2,CN3,CN5,CN6,CN7,CN8
COMPLEX DN(999),S2,S3,S4,S5,CN1,CN4
EXTERNAL FILON
OPEN(16,FILE='DAT.6')
WRITE(*,*) 'ENTER THE FREQUENCY(REAL) IN MHZ'
READ(*,*) FR
WRITE(*,*) ' ENTER THE FIRST SLIT ANGLE(REAL) IN DEGREES'
READ(*,*) TA
WRITE(*,*) 'ENTER SECOND SLIT ANGLE(REAL) IN DEGREES'
READ(*,*) TB
WRITE(*,*) 'ENTER NMAX(INTEGER)'
READ(*,*)NMAX
TP1=TA/57.29578
TP2=TB/57.29578
PI=3.1415927
DTR=PI/180.
i=(0,1)
K=PI*FR/150.
L=300./FR
B=.6*L
A=.5*L
K1=K*B
K1D=DBLE(K1)
K2=K*A
K2D=DBLE(K2)
M=98
H=ABS(TP2-TP1)/FLOAT(M)
CB1=(8.*K1**2-8.*i*K1)/(8.*K1**2-12.*i*K1-3.)
CA1=-(8.*K2**2-8.*i*K2)/(8.*K2**2-12.*i*K2-3.)
CB2=-4./(8.*K1**2-12.*i*K1-3.)
CA2=-4./(8.*K2**2-12.*i*K2-3.)
CALL BES(NMAX,K1D,J,Y,DJ,DY)
CALL BES(NMAX,K2D,J1,Y1,DJ1,DY1)

```

C PLOTTING ROUTINE

```

WRITE(16,960) 'TE CASE PEC SLIT CYLINDER SCATTERING WIDTH '

```

```

NPFI=91
PHI1=0.
PHI2=180.
WRITE(16,970) NPFI
WRITE(16,980) PHI1
WRITE(16,980) PHI2
DO 50 P =0.,180.,2.
    PHI=DTR*P
    IF(P.EQ.0.) THEN
        T1=i*K*(A-B)*COS(TP2)
        T3=i*K*(A-B)*COS(TP1)
    ELSE
        T1=COS(TP2)/(COS(TP2)-COS(TP2+PHI))*(EXP(i*K2*(COS(TP2)-COS(TP2+
        + PHI)))-EXP(i*K1*(COS(TP2)-COS(TP2+PHI))))
        T3=COS(TP1)/(COS(TP1)-COS(TP1+PHI))*(EXP(i*K2*(COS(TP1)-COS(TP1+
        + PHI)))-EXP(i*K1*(COS(TP1)-COS(TP1+PHI))))
    ENDIF
T2=EXP((-i)*K2*COS(TP2+PHI))-EXP((-i)*K1*COS(TP2+PHI))
T4=EXP((-i)*K2*COS(TP1+PHI))-EXP((-i)*K1*COS(TP1+PHI))
C   EVALUATING 1ST FUNCTION F(U)
    DO 100 U =1,M+1
        UU=TP1+(H*(U-1.))
        F(U)=COS(K1*COS(UU+PHI))
100   CONTINUE
        S1=(0,0)
        P1=0.
        DO 200 N=1,NMAX+1
            NMX=FLOAT(N)-1.
            IF(NMX.EQ.0.) THEN
                EN=1.
            ELSE
                EN=2.
            ENDIF
            P2=(0,0)
            P1 = FILON(F,NMX,TP1,TP2,M+1,99,1)
            WRITE(*,*) NMX,P1
            P2=EN*i**NMX*DJ(NMX)
            WRITE(*,*) P2
            P3=P1*P2
            WRITE(*,*) P3
            S1 = S1 + P3
200   CONTINUE
        C1=S1
C   EVALUATING 2ND FUNCTION F(U) (CN2=C1-jC2) & CN4

```

```

DO 250 U=1,M+1
  UU=TP1+(H*(U-1.))
  F(U)=SIN(K1*COS(UU+PHI))
250 CONTINUE
  S1=(0,0)
  S2=(0,0)
  P1=0.
  DO 300 N=1,NMAX+1
    NMX=FLOAT(N)-1.
    S3=(0,0)
    S4=(0,0)
    P2=(0,0)
    IF(NMX.EQ.0.) THEN
      EN=1.
    ELSE
      EN=2.
    ENDIF
    P1=FILON(F,NMX,TP1,TP2,M+1,99,1)
    S3=(-1.)*NMX*J1(NMX)*DJ1(NMX)
    S4=(-1.)*NMX*i**(-1.)*CA1*DJ1(NMX)**2/(1.+CA2*NMX**2)
    DN(N)=2.*PI*EN*(S3-S4)*COS(NMX*PHI)
    P2=EN*i**NMX*DJ(NMX)
    P3=P1*P2
    S1=S1+P3
    S2=S2+DN(N)
300 CONTINUE
    CN4=S2
    C2=S1
    CN2=C1-i*C2

```

C EVALUATING 3RD FUNCTION F(U) & CN7

```

DO 350 U=1,M+1
  UU=TP1+(H*(U-1.))
  F(U)=COS(UU+PHI)*COS(K1*COS(UU+PHI))
350 CONTINUE
  S1=(0,0)
  S2=(0,0)
  P1=0.
  DO 400 N=1,NMAX+1
    NMX=FLOAT(N)-1.
    S3=(0,0)
    S4=(0,0)
    S5=(0,0)
    P2=(0,0)
    IF(NMX.EQ.0.) THEN
      EN=1.
    ELSE
      EN=2.
    ENDIF
    P1=FILON(F,NMX,TP1,TP2,M+1,99,1)
    P2=EN*CB1*i**(-NMX-1.)*(-1.)*NMX*DJ(NMX)/(1.+CB2*NMX**2)

```

```

S3=COS(NMX*TP2)*T2
S4=(CB1*i**(-NMX-1.)*DJ(NMX))/(1.+CB2*NMX**2)
S5=(CA1*i**(-NMX-1.)*DJ1(NMX))/(1.+CA2*NMX**2)
DN(N)=EN/2.*(-1.)**NMX*(S4+S5)*S3
P3=P1*P2
S1=S1+P3
S2=S2+DN(N)
400 CONTINUE
C3=S1
CN7=S2

```

C EVALUATING 4RTH FUNCTION (CN3=C3-jc4) & CN8

```

DO 450 U=1,M+1
UU=TP1+(H*(U-1.))
F(U)=COS(UU+PHI)*SIN(K1*COS(UU+PHI))
450 CONTINUE
S1=(0,0)
S2=(0,0)
P1=0.
DO 500 N=1,NMAX+1
NMX=FLOAT(N)-1.
S3=(0,0)
S4=(0,0)
S5=(0,0)
P2=(0,0)
IF(NMX.EQ.0.) THEN
EN=1.
ELSE
EN=2.
ENDIF
P1=FILON(F,NMX,TP1,TP2,M+1,99,1)
P2=EN*CB1*i**(-NMX-1.)*(-1.)**NMX*DJ(NMX)/(1.+CB2*NMX**2)
P3=P1*P2
S3=COS(NMX*TP1)*T4
S4=(CB1*i**(-NMX-1.)*DJ(NMX))/(1.+CB2*NMX**2)
S5=(CA1*i**(-NMX-1.)*DJ1(NMX))/(1.+CA2*NMX**2)
DN(N)=EN/2.*(-1.)**NMX*(S4+S5)*S3
S1=S1+P3
S2=S2+DN(N)
500 CONTINUE
CN8=S2
C4=S1
CN3=C3-i*C4

```

C EVALUATING 5TH FUNCTION

```

DO 550 U=1,M+1
UU=TP1+(H*(U-1.))
F(U)=COS(K2*COS(UU+PHI))
550 CONTINUE
S1=(0,0)
P1=0.

```

```

DO 600 N=1,NMAX+1
NMX=FLOAT(N)-1.
IF(NMX.EQ.0.) THEN
EN=1.
ELSE
EN=2.
ENDIF
P2=(0,0)
P1=FILON(F,NMX,TP1,TP2,M+1,99,1)
P2=EN*i**NMX*DJ1(NMX)
P3=P1*P2
S1=S1+P3
600 CONTINUE
C5=S1

C EVALUATING 6TH FUNCTION (CN5=C5-jC6)
DO 650 U=1,M+1
UU=TP1+(H*(U-1.))
F(U)=SIN(K2*COS(UU+PHI))
650 CONTINUE
S1=(0,0)
P1=0.
DO 700 N=1,NMAX+1
NMX=FLOAT(N)-1.
IF(NMX.EQ.0.) THEN
EN=1.
ELSE
EN=2.
ENDIF
P2=(0,0)
P1=FILON(F,NMX,TP1,TP2,M+1,99,1)
P2=EN*i**NMX*DJ1(NMX)
P3=P1*P2
S1=S1+P3
700 CONTINUE
C6=S1
CN5=C5+i*C6

C EVALUATING THE 7TH FUNCTION & CN1
DO 750 U=1,M+1
UU=TP1+(H*(U-1.))
F(U)=COS(UU+PHI)*COS(K2*COS(UU+PHI))
750 CONTINUE
S1=(0,0)
S2=(0,0)
P1=0.
DO 800 N=1,NMAX+1
NMX=FLOAT(N)-1.
S3=(0,0)
S4=(0,0)
IF(NMX.EQ.0.) THEN
EN=1.

```

```

        ELSE
        EN=2.
        ENDIF
        P2=(0,0)
        P1=FILON(F,NMX,TP1,TP2,M+1,99,1)
P2=EN*CA1*i**(-NMX-1.)*(-1.)**NMX*DJ1(NMX)/(1.+CA2*NMX**2)
        S3=J(NMX)*DJ(NMX)
        S4=i**(-1)*CB1*DJ(NMX)**2/(1+CB2*NMX**2)
        DN(N)=2.*PI*EN*(S3+S4)*COS(NMX*PHI)
        P3=P1*P2
        S1=S1+P3
        S2=S2+DN(N)
800      CONTINUE
        C7=S1
        CN1=S2

C      EVALUATING THE 8TH FUNCTION (CN6=C7-jC8)
        DO 850 U=1,M+1
            UU=TP1+(H*(U-1.))
            F(U)=COS(UU+PHI)*SIN(K2*COS(UU+PHI))
850      CONTINUE
            S1=(0,0)
            P1=0.
            DO 900 N=1,NMAX+1
                NMX=FLOAT(N)-1.
                IF(NMX.EQ.0.) THEN
                    EN=1.
                ELSE
                    EN=2.
                ENDIF
                P2=(0,0)
                P1=FILON(F,NMX,TP1,TP2,M+1,99,1)
                P2=EN*CA1*i**(-NMX-1.)*(-1.)**NMX*DJ1(NMX)/(1.+CA2*NMX**2)
                P3=P1*P2
                S1=S1+P3
900      CONTINUE
                C8=S1
                CN6=C7+i*C8
                SIGMA=1./(8.*PI)*CABS(-K1*(CN1-CN2+i*CN3)-K2*(CN4-CN5+i*CN6)
+                -T1-T3+CN7+CN8)**2
                SIG=(SIGMA)**.5
                WRITE(16,980) SIG
50      CONTINUE
            CLOSE(16)
960      FORMAT(A)
970      FORMAT(I5)
980      FORMAT(E12.3)
        STOP
        END

```

**APPENDIX F. PROGRAM TO COMPUTE  $\sigma/\pi b$  versus KB FOR SLIT  
CIRCULAR CYLINDERS**

C THIS PROGRAM COMPUTES THE SCATTERING WIDTH/ $\pi b$  FOR A CIRCULAR  
C CIRCULAR HOLLOW CYLINDER WITH A SLIT OF ANY SIZE FOR THE  
C TRANSVERSE ELECTRIC POLARIZATION CASE USING THE ON - SURFACE  
C RADIATION CONDITION APPROACH .

```

REAL*8 J(0:200),Y(0:200),DY(0:200),DJ(0:200),K1D,K2D
REAL*8 J1(0:200),Y1(0:200),DJ1(0:200),DY1(0:200),H1
REAL EN,NMX,R,U,UU,H,P,PI,PHI,F(99),P1
INTEGER M,N,NT,NMAX
REAL TA,TB,K,K1,K2,TP1,TP2,FILON,FR,B,A,L
COMPLEX P2,P3,i,S1,T1,T2,T3,T4,CB1,CB2,CA1,CA2
COMPLEX C1,C2,C3,C4,C5,C6,C7,C8,CN2,CN3,CN5,CN6,CN7,CN8
COMPLEX DN(99),S2,S3,S4,S5,CN1,CN4
EXTERNAL FILON
OPEN(3,FILE='DAT.71')
WRITE(*,*) 'ENTER THE PHI ANGLE(REAL) IN DEGREES '
READ(*,*) P
WRITE(*,*) 'ENTER THE OUTER RADIUS(REAL) IN METERS '
READ(*,*) B
WRITE(*,*) 'ENTER THE INNER RADIUS(REAL) IN METERS '
READ(*,*) A
WRITE(*,*) ' ENTER THE FIRST SLIT ANGLE(REAL) IN DEGREES '
READ(*,*) TA
WRITE(*,*) 'ENTER SECOND SLIT ANGLE(REAL) IN DEGREES '
READ(*,*) TB
WRITE(*,*) 'ENTER NMAX(INTEGER) '
READ(*,*) NMAX
TP1=TA/57.29578
TP2=TB/57.29578
PI=3.1415927
DTR=PI/180.
PHI=P*DTR
i=(0,1)
M=98
H=ABS(TP2-TP1)/FLOAT(M)

```

C PLOTTING ROUTINE

```

WRITE(3,960) 'TE CASE PEC SLIT CYLINDER SCATTERING WIDTH '
NPHI=59
PHI1=0.1
PHI2=6.
WRITE(3,970) NPHI
WRITE(3,980) PHI1
WRITE(3,980) PHI2
DO 50 R =0.1,6.,.1
    K1=R*B
    K2=R*A
    K1D=DBLE(K1)
    K2D=DBLE(K2)
    CB1=(8.*K1**2-8.*i*K1)/(8.*K1**2-12.*i*K1-3.)
    CA1=- (8.*K2**2-8.*i*K2)/(8.*K2**2-12.*i*K2-3.)

```

```

CB2=-4./(8.*K1**2-12.*i*K1-3.)
CA2=-4./(8.*K2**2-12.*i*K2-3.)
CALL BES(NMAX,K1D,J,Y,DJ,DY)
CALL BES(NMAX,K2D,J1,Y1,DJ1,DY1)
IF(P.EQ.0.) THEN
T1=i*K*(A-B)*COS(TP2)
T3=i*K*(A-B)*COS(TP1)
ELSE

```

```

T1=COS(TP2)/(COS(TP2)-COS(TP2+PHI))*(EXP(i*K2*(COS(TP2)-COS(TP2+
+ PHI)))-EXP(i*K1*(COS(TP2)-COS(TP2+PHI))))

```

```

T3=COS(TP1)/(COS(TP1)-COS(TP1+PHI))*(EXP(i*K2*(COS(TP1)-COS(TP1+
+ PHI)))-EXP(i*K1*(COS(TP1)-COS(TP1+PHI))))

```

```

ENDIF

```

```

T2=EXP((-i)*K2*COS(TP2+PHI))-EXP((-i)*K1*COS(TP2+PHI))

```

```

T4=EXP((-i)*K2*COS(TP1+PHI))-EXP((-i)*K1*COS(TP1+PHI))

```

### C EVALUATING 1ST FUNCTION F(U)

```

DO 100 U =1,M+1
    UU=TP1+(H*(U-1.))
    F(U)=COS(K1*COS(UU+PHI))
100 CONTINUE
    S1=(0,0)
    P1=0.
    DO 200 N=1,NMAX+1
        NMX=FLOAT(N)-1.
        IF(NMX.EQ.0.) THEN
            EN=1.
        ELSE
            EN=2.
        ENDIF
        P2=(0,0)
        P1 = FILON(F,NMX,TP1,TP2,M+1,99,1)
        WRITE(*,*) NMX,P1
        P2=EN*i**NMX*J(NMX)
        H1=J(NMX)
        WRITE(*,*) P2
        P3=P1*P2
        WRITE(*,*) P3
        S1 = S1 + P3
200 CONTINUE
    C1=S1

```

### C EVALUATING 2ND FUNCTION F(U) (CN2=C1-jC2) & CN4

```

DO 250 U=1,M+1
    UU=TP1+(H*(U-1.))
    F(U)=SIN(K1*COS(UU+PHI))

```

250

CONTINUE

S1=(0,0)

S2=(0,0)

P1=0.

DO 300 N=1,NMAX+1

NMX=FLOAT(N)-1.

S3=(0,0)

S4=(0,0)

P2=(0,0)

IF(NMX.EQ.0.) THEN

EN=1.

ELSE

EN=2.

ENDIF

P1=FILON(F,NMX,TP1,TP2,M+1,99,1)

S3=(-1.)\*NMX\*J1(NMX)\*DJ1(NMX)

S4=(-1.)\*NMX\*i\*\*(-1.)\*CA1\*DJ1(NMX)\*\*2/(1.+CA2\*NMX\*\*2)

DN(N)=2.\*PI\*EN\*(S3-S4)\*COS(NMX\*PHI)

P2=EN\*i\*\*NMX\*J(NMX)

P3=P1\*P2

S1=S1+P3

S2=S2+DN(N)

CONTINUE

CN4=S2

C2=S1

CN2=C1-i\*C2

300

C EVALUATING 3RD FUNCTION F(U) &amp; CN7

DO 350 U=1,M+1

UU=TP1+(H\*(U-1.))

F(U)=COS(UU+PHI)\*COS(K1\*COS(UU+PHI))

350

CONTINUE

S1=(0,0)

S2=(0,0)

P1=0.

DO 400 N=1,NMAX+1

NMX=FLOAT(N)-1.

S3=(0,0)

S4=(0,0)

S5=(0,0)

P2=(0,0)

IF(NMX.EQ.0.) THEN

EN=1.

ELSE

EN=2.

ENDIF

P1=FILON(F,NMX,TP1,TP2,M+1,99,1)

P2=EN\*CB1\*i\*\*(-NMX-1.)\*(-1.)\*NMX\*DJ(NMX)/(1.+CB2\*NMX\*\*2)

S3=COS(NMX\*TP2)\*T2

S4=(CB1\*i\*\*(-NMX-1.)\*DJ(NMX))/(1.+CB2\*NMX\*\*2)

```

S5=(CA1*i**(-NMX-1.)*DJ1(NMX))/(1.+CA2*NMX**2)
DN(N)=EN/2.*(-1.)**NMX*(S4+S5)*S3
P3=P1*P2
S1=S1+P3
S2=S2+DN(N)
400 CONTINUE
C3=S1
CN7=S2

```

C EVALUATING 4RTH FUNCTION (CN3=C3-jC4) & CN8

```

DO 450 U=1,M+1
UU=TP1+(H*(U-1.))
F(U)=COS(UU+PHI)*SIN(K1*COS(UU+PHI))
450 CONTINUE
S1=(0,0)
S2=(0,0)
P1=0.
DO 500 N=1,NMAX+1
NMX=FLOAT(N)-1.
S3=(0,0)
S4=(0,0)
S5=(0,0)
P2=(0,0)
IF(NMX.EQ.0.) THEN
EN=1.
ELSE
EN=2.
ENDIF
P1=FILON(F,NMX,TP1,TP2,M+1,99,1)
P2=EN*CB1*i**(-NMX-1.)*(-1.)**NMX*DJ(NMX)/(1.+CB2*NMX**2)
P3=P1*P2
S3=COS(NMX*TP1)*T4
S4=(CB1*i**(-NMX-1.)*DJ(NMX))/(1.+CB2*NMX**2)
S5=(CA1*i**(-NMX-1.)*DJ1(NMX))/(1.+CA2*NMX**2)
DN(N)=EN/2.*(-1.)**NMX*(S4+S5)*S3
S1=S1+P3
S2=S2+DN(N)
500 CONTINUE
CN8=S2
C4=S1
CN3=C3-i*C4

```

C EVALUATING 5TH FUNCTION

```

DO 550 U=1,M+1
UU=TP1+(H*(U-1.))
F(U)=COS(K2*COS(UU+PHI))
550 CONTINUE
S1=(0,0)
P1=0.
DO 600 N=1,NMAX+1
NMX=FLOAT(N)-1.

```

```

        IF(NMX.EQ.0.) THEN
        EN=1.
        ELSE
        EN=2.
        ENDIF
        P2=(0,0)
        P1=FILON(F,NMX,TP1,TP2,M+1,99,1)
        P2=EN*i**NMX*J1(NMX)
        P3=P1*P2
        S1=S1+P3
600      CONTINUE
        C5=S1

C      EVALUATING 6TH FUNCTION (CN5=C5-jC6)
        DO 650 U=1,M+1
            UU=TP1+(H*(U-1.))
            F(U)=SIN(K2*COS(UU+PHI))
650      CONTINUE
            S1=(0,0)
            P1=0.
            DO 700 N=1,NMAX+1
                NMX=FLOAT(N)-1.
                IF(NMX.EQ.0.) THEN
                EN=1.
                ELSE
                EN=2.
                ENDIF
                P2=(0,0)
                P1=FILON(F,NMX,TP1,TP2,M+1,99,1)
                P2=EN*i**NMX*J1(NMX)
                P3=P1*P2
                S1=S1+P3
700      CONTINUE
            C6=S1
            CN5=C5-i*C6

C      EVALUATING THE 7TH FUNCTION & CN1
        DO 750 U=1,M+1
            UU=TP1+(H*(U-1.))
            F(U)=COS(UU+PHI)*COS(K2*COS(UU+PHI))
750      CONTINUE
            S1=(0,0)
            S2=(0,0)
            P1=0.
            DO 800 N=1,NMAX+1
                NMX=FLOAT(N)-1.
                S3=(0,0)
                S4=(0,0)
                IF(NMX.EQ.0.) THEN
                EN=1.
                ELSE
                EN=2.

```

```

        ENDIF
        P2=(0,0)
        P1=FILON(F,NMX,TP1,TP2,M+1,99,1)
P2=EN*CA1*i**(-NMX-1.)*(-1.)**NMX*DJ1(NMX)/(1.+CA2*NMX**2)
        S3=J(NMX)*DJ(NMX)
        S4=i**(-1)*CB1*DJ(NMX)**2/(1+CB2*NMX**2)
DN(N)=2.*PI*EN*(S3+S4)*COS(NMX*PHI)
        P3=P1*P2
        S1=S1+P3
        S2=S2+DN(N)
800      CONTINUE
        C7=S1
        CN1=S2

C      EVALUATING THE 8TH FUNCTION (CN6=C7-jc8)
      DO 850 U=1,M+1
        UU=TP1+(H*(U-1.))
        F(U)=COS(UU+PHI)*SIN(K2*COS(UU+PHI))
850      CONTINUE
        S1=(0,0)
        P1=0.
      DO 900 N=1,NMAX+1
        NMX=FLOAT(N)-1.
        IF(NMX.EQ.0.) THEN
          EN=1.
        ELSE
          EN=2.
        ENDIF
        P2=(0,0)
        P1=FILON(F,NMX,TP1,TP2,M+1,99,1)
P2=EN*CA1*i**(-NMX-1.)*(-1.)**NMX*DJ1(NMX)/(1.+CA2*NMX**2)
        P3=P1*P2
        S1=S1+P3
900      CONTINUE
        C8=S1
        CN6=C7-i*C8

SIGMA=1./(4.*K1*PI)*CABS(-K1*(CN1-CN2+i*CN3)-K2*(CN4-CN5+i*CN6)
+
        -T1-T3+CN7+CN8)**2

      WRITE(3,980) SIGMA
50      CONTINUE
      CLOSE(3)
960      FORMAT(A)
970      FORMAT(I5)
980      FORMAT(E12.3)
STOP
END

```

## APPENDIX G. PROGRAM TO COMPUTE THE BESSEL FUNCTIONS

```

SUBROUTINE BES(N,X,J,Y,DJ,DY)
C   THIS SUBROUTINE WAS OBTAINED DURING EC 4600 FROM PROFESSOR
C   MICHAEL A. MORGAN.
C   Double precision calculation of ordinary Bessel functions,
C   Jn(X)
C   and Yn(X), and their first derivative, DJ and DY, for integer
C
C   order "n" from n=0 to N with real argument X.
C
REAL*8 J(0:200),Y(0:200),DJ(0:200),DY(0:200),SCALE,JTEMP2,X
REAL*8 SCLFAC,A,B,C,D,E,F,PI,JTEMP,JTEMP1
PI=3.14159265359D0
IF (X.EQ.0.0D00) THEN
C   X = 0.0 BOUNDARY CASE
      IF (N.EQ.1) THEN
          J(1) = 0.0D00
          DJ(1) = 0.5D00
      ELSE
          DO 5, I = N, 2, -1
              J(I) = 0.0D00
              DJ(I) = 0.0D00
          5      CONTINUE
          J(1) = 0.0D00
          DJ(1) = 0.5D00
          ENDIF
          J(0) = 1.0D00
          DJ(0) = 0.0D00
          Y(N) = -1.0D-300
          DY(N) = 1.0D300
      ELSEIF (N.EQ.0) THEN
C   POLYNOMIAL EXPANSION ONLY FOR N = 0
          CALL BES0(X,J,Y,PI,DJ,DY)
      ELSE
C   RECURSION FOR ALL OTHER CASES
C   Y IS A FORWARD RECURSION
          CALL BES0(X,J,Y,PI,DJ,DY)
          Y(1) = -DY(0)
          DY(1)=Y(0) - Y(1)/X
          IF (N.EQ.1) GO TO 20
          DO 10, I = 0, N-2
              Y(I+2) = (2.0D00*(I+1)/X)*Y(I+1) - Y(I)
              DY(I+2) = Y(I+1) - ((I+2)/X)*Y(I+2)
          10      CONTINUE
C   J IS A REVERSE RECURSION BASED ON A PAIR OF BESSEL FUNCTION
C   POINTS DERIVED FROM A TRUNCATED POWER SERIES EXPANSION. THE
C   RECURSION IS THEN SCALED TO A KNOWN VALUE, J1(X).
          20      SCALE = -DJ(0)
          NSAVE = N
          IF (X.LE.N) THEN
              N = 5*N+50

```

```

        GOTO 25
    ENDIF
    N = IDNINT(N + X*X + 0.5D00)
C
25    A = 1.0D00/DFLOAT(N+1)
    B = 1.0D00/DFLOAT(N+2)
    C = 1.0D00/DFLOAT(N+3)
    D = 1.0D00/DFLOAT(N+4)
    E = 1.0D00/DFLOAT(N+5)
    F = X/2.0D00
C
    JTEMP = 1-A**2+0.5D00*A*B**4-(1.0D00/6.0D00)*A*B*C**6+
+(1.0D00/24.0D00)*A*B*C*D**8-(1.0D00/120.0D00)*A**3*C*D**10
C
    N = N - 1
    A = 1.0D00/DFLOAT(N+1)
    B = 1.0D00/DFLOAT(N+2)
    C = 1.0D00/DFLOAT(N+3)
    D = 1.0D00/DFLOAT(N+4)
    E = 1.0D00/DFLOAT(N+5)
    F = X/2.0D00
C
    JTEMP1 = 1-A**2+0.5D00*A*B**4-(1.0D00/6.0D00)*A*B*C**6+
+(1.0D00/24.0D00)*A*B*C*D**8-(1.0D00/120.0D00)*A**3*C*D**10
C
    DO 30, I = N+1,2,-1
    JTEMP = 2*((I - 1)/X)*JTEMP1 - JTEMP
    IF(DABS(JTEMP).GE.1.0D250) THEN
        JTEMP2 = JTEMP*1.0D-250
        JTEMP1 = JTEMP*1.0D-250
    ENDIF
    JTEMP = JTEMP1
    JTEMP1 = JTEMP2
    IF ((I-2).LE.NSAVE) THEN
        J(I-2) = JTEMP2
    ENDIF
30    CONTINUE
C
    SCALING
    N = NSAVE
    SCLFAC = SCALE/J(1)
    DO 40, I = 0, N
    J(I) = SCLFAC*J(I)
    IF (I.EQ.0) THEN
        GOTO 40
    ENDIF
    IF (ABS(J(I)/J(I-1)).LT.1.0D-50) THEN
        J(I) = J(I)*1.0D250
    ELSEIF (ABS(J(I)/J(I-1)).GT.1.0D50) THEN
        J(I) = J(I)*1.0D-250
    ENDIF

```

```

40    DJ(I) = J(I-1) - (I/X)*J(I)
      CONTINUE
      ENDIF
      RETURN
      END

C
      SUBROUTINE BES0(X,J,Y,PI,DJ,DY)
C      FOR ZERO ORDER BESSEL FUNCTIONS ONLY
      DIMENSION J(0:200), Y(0:200), DJ(0:200), DY(0:200)
      DOUBLE PRECISION J, Y, X, PI, DJ, DY, F0, F1, THETA0
      DOUBLE PRECISION THETA1, A
      IF (X.LE.3.0D00) THEN
      A = X/3.0D00
      J(0) = 1.0D00 - 2.2499997D00*(A**2) +
1.2656208D00*(A**4) -
      +0.3163866D00*(A**6) + 0.0444479D00*(A**8) -
0.0039444D00*(A**10) +
      +0.00021D00*(A**12)
      Y(0) = (2.0D00/PI)*DLOG(X/2.0D00)*J(0) + 0.36746691D00
+
      +.60559366D00*(A**2) - 0.74350384D00*(A**4) +
0.25300117D00*(A**6)
      + - 0.04261214D00*(A**8) + 0.00427916D00*(A**10) -
0.00024846D00*
      + (A**12)
      DJ(0)=-X*(.5D00-0.56249985D00*(A**2)+0.21093573D00
      +(A**4)- 0.03954289D00*(A**6) + 0.00443319D00*(A**8) -
0.00031761
      +D00*(A**10) + 0.00001109D00*(A**12))
      D Y ( 0 ) =
(-1.0D00/X)*((2.0D00/PI)*X*DLOG(X/2D00)*(-1.0D00*
      +DJ(0))-0.6366198D00+0.2212091D00*(A**2)+2.1682709D00*(A**4)
-
      +1.3164827D00*(A**6) + 0.3123951D00*(A**8) -
0.0400976D00*(A**10)
      + + 0.0027873D00*(A**12))
      ELSE
      A = 3.0D00/X
      F0 = .79788456D00 - 0.00000077D00*A -
0.00552740D00*(A**2)
      +-0.00009512D00*(A**3) + 0.00137237D00*(A**4)
-0.00072805D00*(A**5)
      ++0.00014476D00*(A**6)
      THETA0 = X - 0.78539816D00 - 0.04166397D00*A -
0.00003954
      +D00*(A**2) + 0.00262573D00*(A**3) - 0.00054125D00*(A**4) -
      +0.00029333D00*(A**5) + 0.00013558D00*(A**6)
      J(0) = F0*DCOS(THETA0)/DSQRT(X)
      Y(0) = F0*DSIN(THETA0)/DSQRT(X)
      F1 = 0.79788456D00 + 0.00000156D00*A + 0.01659667D00*A*A
      ++0.00017105D00*(A**3) - 0.00249511D00*(A**4) + 0.00113653D00
      +(A**5) -0.00020033D00*(A**6)

```

```
      THETA1 = X - 2.35619449D00 + .12499612D00*A + 0.00005650
+D00*(A**2) - 0.00637879D00*(A**3) + 0.00074348D00*(A**4) +
+ 0.00079824D00*(A**5) - 0.00029166D000*(A**6)
      DJ(0) = -F1*DCOS(THETA1)/DSQRT(X)
      DY(0) = -F1*DSIN(THETA1)/DSQRT(X)
ENDIF
RETURN
END
```



```

2      IF (T .EQ. 0.) THEN
      FILON = 0.
      RETURN
      END IF
      SU = F1 * C1 - F2 * C2
      SU1 = -0.5 * (F2 * S2 - F1 * S1)
      DO 5 I = 2, N, 2
      SUM = SUM + F (I) * SIN (A1 * T)
      A1 = A1 + H
      SU1 = SU1 + F (I+1) * SIN (A1 * T)
5      A1 = A1 + H
4      FILON = H * (AL * SU + BE * SU1 + GA * SUM)
      RETURN
      END

```

## LIST OF REFERENCES

1. G. A. Kriegsman and A. Taflove, "A new formulation of EM wave scattering using an On-Surface Radiation Boundary Condition Approach", IEEE Trans. Antennas and Propagation, Vol. AP-35, pp. 153-161, No.2 February 1987.
2. D. K. Cheng, Field and Wave Electromagnetics, New York: Wesley, 1989.
3. G. B. Thomas and R. L. Finley, Calculus and Analytic Geometry, Reading, Massachusetts: Wesley, 1980.
4. D. Berkey, Calculus, New York: Saunders, 1988.
5. R. W. Ziolkowski and J. B. Grant, "Scattering from cavity-backed Apertures: The generalized dual series solution of the cocentrically loaded E-Pol slit cylinder problem", IEEE Trans. Antennas and Propagation, Vol. AP-35, pp. 504-528, No.5 May 1987.
6. J. Van Bladel, Electromagnetic Fields, New York: McGraw-Hill, 1980.
7. M. G. Andreasen, "Scattering from parallel metallic cylinders with arbitrary cross sections", IEEE Trans. Antennas and Propagation, pp. 746-754, November 1964.
8. C.R. Mullin, R. Sandburg and C.O. Velline, "A numerical technique for the determination of scattering cross sections of infinite cylinders of arbitrary geometrical cross section", IEEE Trans. Antennas and Propagation, pp. 141-149, January 1965.

9. J. J. Bowman, T. B. A. Senior and P. L. E. Uslenghi, Electromagnetic and Acoustic Scattering by Simple Shapes, Amsterdam: North-Holland, 1969.

10. W. H. Beyer, CRC Standard Mathematical Tables, Florida: CRC Press, 1987.

**INITIAL DISTRIBUTION LIST**

	No. Copies
1. Defense Technical Information Center Cameron Station Alexandria, VA 22304-6145	1
2. Library, Code 52 Naval Postgraduate School Monterey, CA 93943-5002	1
3. Department Chairman, Code EC Department of Electrical and Computer Engineering Naval Postgraduate School Monterey, CA 93943-5000	1
4. Professor Rama Janaswamy, Code EC/Js Department of Electrical and Computer Engineering Naval Postgraduate School Monterey, CA 93943-5000	1
5. Director Research Administration, Code 81 Naval Postgraduate School Monterey, CA 93843-5000	1
6. Chief of The Naval Staff Naval Headquarters, Islamabad Pakistan	1
7. Assistant Chief of Naval Staff (Technical Services) Naval Headquarters, Islamabad Pakistan	1
8. Assistant Chief of Naval Staff (Training) Naval Headquarters, Islamabad Pakistan	1
9. Commander Pakistan Fleet c/o Fleet Mail Office at P.N.S. Haider, Karachi, Pakistan	1
10. Commander Karachi c/o Fleet Mail Office 10 Liaquat Barracks Shara-e-Faisal, Karachi, Pakistan	1

- |                                                                                                                                                |   |
|------------------------------------------------------------------------------------------------------------------------------------------------|---|
| 11. Commander Logistics<br>c/o Fleet Mail Office<br>P.N.S. Peshawar<br>PN Dockyard, Karachi, Pakistan                                          | 1 |
| 12. Director Naval Weapons and Engineering<br>Naval Headquarters, Islamabad<br>Pakistan                                                        | 1 |
| 13. Director Ships Maintenance and Repairs<br>Naval Headquarters, Islamabad<br>Pakistan                                                        | 1 |
| 14. Naval Attache Pakistan<br>Embassy of Pakistan<br>2201 R Street, N.W.<br>Washington DC 20008                                                | 1 |
| 15. Commanding Officer<br>P.N.S. Karsaz<br>Shara-e-Faisal<br>Karachi, Pakistan                                                                 | 1 |
| 16. Commanding Officer<br>PN Engineering College<br>P.N.S. Jauhar<br>Ibrahim Rehmatullah Road<br>Karachi, Pakistan                             | 1 |
| 17. Dr. Richard W. Adler, Code EC/Ab<br>Department of Electrical and Computer Engineering<br>Naval Postgraduate School<br>Monterey, CA 939 000 | 1 |
| 18. Lieutenant Commander Syed Mahmood Ali<br>c/o PN Engineering College<br>P.N.S. Jauhar<br>Ibrahim Rehmatullah Road<br>Karachi, Pakistan      | 2 |